UCRL-16824

University of California
Ernest O. Lawrence Radiation Laboratory

CORRELATIONS OF PHOTONS FROM A THERMAL SOURCE

Berkeley, California

DISCLAIMER

Special Thesis

UCRL-16824

UNIVERSITY OF CALIFORNIA

Lawrence Radiation Laboratory
Berkeley, California

AEC Contract No. W-7405-eng-48

CORRELATIONS OF PHOTONS FROM A THERMAL SOURCE

Shang-keng Ma
(Ph. D. Thesis)

April 21, 1966

Contents

CORRELATION OF PHOTONS FROM A THERMAL SOURCE

Shang-keng Ma

Lawrence Radiation Laboratory
University of California
Berkeley, California

April 21, 1966

ABSTRACT

The amplitude and the intensity-correlation of photons from a model thermal source are studied. The objective is to express the photon correlation functions in terms of the parameters describing the source. The source model is analyzed utilizing the temperature Green's function method. The power spectrum (line shape) is computed numerically for some special cases. General properties of temperature Green's functions are also studied.

I. INTRODUCTION

The electromagnetic field in the vacuum outside a light source is determined by the processes in the source. Therefore, the analysis of the statistical properties of a beam of photons involves a study of the stochastic processes in the source.

For all practical purposes, most of the useful information concerning a beam of photons is contained in the amplitude- and the intensity-correlation functions. The former is the average of the product of the field amplitudes at two space time points, and, the later, that of the intensities at two space time points.

These correlation functions, and more general ones, have been studied by many authors without explicitly treating the emission processes in the source within the framework of classical electromagnetic theory,[1] in terms of many body wave functions,[2] and in terms of the eigenstates of the annihilation operators.[3] On the other hand, the explicit treatment of photon emission process can be found in the papers on the theories of the spectral line shape, which have a very long history.[4] The spectral line shape theories in general deal with a single emitter under the perturbation due to its environment while a photon is being emitted.

The scope of this thesis is the following. We shall study the photon field and the source coupled together. The source is viewed as a many body system. The correlations in this many body system give rise to the correlations in the photon field. To make the over-all picture clear, we shall construct an idealized model for the source. This source model is then analyzed by the temperature Green's function method. The

result of our analysis will be the expressions of the photon correlation functions in terms of the parameters describing the source. General properties of temperature Green's functionsare also studied.

In Chapter II, we clarify the connection between the photon correlations and the correlations in the source. The source model is introduced in Chapter III, where the assumptions are discussed and the mathematical procedure outlined. Chapter IV gives a discussion of some general properties of temperature Green's functions as well as a derivation of some specific equations needed in later analysis. Chapters V and VI are devoted to the analysis of the power spectrum, which is proportional to the Fourier transform of the amplitude correlation function. The analysis is essentially a simple investigation of the emission line shape from a many body viewpoint. A numerical calculation is carried out to compute the power spectrum under more restrictive conditions. Special attention is paid to the collision narrowing phenomenon. We analyze the intensity correlation of photons in terms of a temperature Green's function of three time arguments. The general properties of such a Green's function are studied in Chapter VII. In Chapter VIII, the connection between the intensity correlation function and the three time temperature Green's function is derived. The expression for the intensity correlation function is then derived.

II. BASIC NOTION

A. Definitions

Let the vector $A_\alpha(y)$ be the annihilation operator in the Heisenberg picture for the transverse photon field at the space-time point $y = (\underset{\sim}{y}, t)$. The amplitude and intensity correlation functions are defined respectively as:

$$\text{Amplitude Correlation function} = \langle A^\dagger_\alpha(y_1)\, A_\beta(y_2)\rangle \ , \tag{2-1}$$

Intensity Correlation function

$$= \langle \left(A^\dagger_\alpha(y_1)\, A^\dagger_\beta(y_2)\right)_- \left(A_\beta(y_2)\, A_\alpha(y_1)\right)_+ \rangle \ , \tag{2-2}$$

where $(\ldots)_+$ and $(\ldots)_-$ denote respectively the time ordering and the inverse time ordering of the operators in the bracket. The average $\langle \ldots \rangle$ is taken over the statistical ensemble describing the photon source. While the amplitude correlation function is often used in calculating interference effects, the intensity correlation defined by (2-2), which is seen to be proportional to the probability of finding two photons,* is useful in describing two-photon-experiments such as the coincidence counting experiment.

---

* The probability of finding a photon at y_1 and a photon at y_2 is proportional to

$$\sum_f |\langle f| \left(A_\beta(y_2)\, A_\alpha(y_1)\right)_+ |s\rangle|^2 \ .$$

Our objective is to express these correlation functions in terms of parameters describing the source. Let us first discuss briefly the different approaches appropriate for calculating correlations of photons from different types of sources.

B. The Cavity-Vacuum Coupling

A light source is a bounded region in space, which we shall call the "cavity," and in which photons are created and finally escape into the empty space outside. Let L denote the size of the cavity, and T, $(0 \leqslant T \leqslant 1)$, denote the transmission coefficient of the boundary, then the "cavity width"

$$\Gamma_c \approx T/L \tag{2-3}$$

is the leak rate of a photon after its creation. (We use units such that $\hbar = c = 1$.) A photon inside the cavity is an excitation of a cavity mode oscillator, and a photon outside is an excitation of an oscillation mode of the empty space. Γ_c therefore measures the coupling strength between the cavity and the empty space. Clearly, Γ_c will be small if L is large or T is small or both. Therefore, for a large source or a source with an opaque boundary, the cavity-vacuum coupling is very weak. For these sources, one would treat the photons in the cavity first and then couple the cavity to the vacuum outside by perturbation theory. Stars and lasers are examples of sources with weak vacuum-cavity coupling.

On the other hand, if the source is small and transparent, the cavity-coupling becomes strong according to (2-3). It would be more convenient to couple the atoms in the source directly to the photons in the vacuum outside.

Our source model, which will be described in the next chapter,

will be small and have a transparent boundary; we shall couple the photons outside directly to the atoms. We now write expressions for (2-1) and (2-2) in terms of operators describing the atoms in the source.

C. Expressions in Terms of Current Correlations

If the photons are created by the atoms via an interaction of the form

$$\mathcal{H}(x) = g\, A_\mu^\dagger(x)\, j_\mu(x) + \text{h.c.} \tag{2-4}$$

where g is a constant and $j_\mu(x)$, the current, is a vector appropriately constructed from atomic operators, then it is straightforward to derive the following expressions for the correlation functions: (see Appendix A.)

$$\langle A_\alpha^\dagger(y_1)\, A_\beta(y_2)\rangle$$

$$= |g|^2 \int d^4x_1\, d^4x_2\, D^*_{\alpha\mu}(y_1 - x_1)\, D_{\beta\nu}(y_2 - x_2)\, \langle j_\mu^\dagger(x_1)\, j_\nu(x_2)\rangle\,, \tag{2-5}$$

$$\langle \left(A_\alpha^\dagger(y_1)\, A_\beta^\dagger(y_2)\right)_- \left(A_\beta(y_2)\, A_\alpha(y_1)\right)_+ \rangle$$

$$= |g|^4 \int d^4x_1\, d^4x_2\, d^4x'_1\, d^4x'_2\, D^*_{\alpha\mu}(y_1 - x_1)\, D^*_{\beta\nu}(y_2 - x_2)$$

$$\times\, D_{\beta\nu'}(y_2 - x'_2)\, D_{\alpha\mu'}(y_1 - x'_1)$$

$$\times\, \langle \left(j_\mu^\dagger(x_1)\, j_\nu^\dagger(x_2)\right)_- \left(j_{\nu'}(x'_2)\, j_{\mu'}(x'_1)\right)_+ \rangle\,, \tag{2-6}$$

where $D_{\alpha\beta}(y - x)$ is the retarded commutator: (see (A-6))

$$D_{\alpha\beta}(y - x) = \theta(t - \tau)\,[A'_\alpha(y),\, A'^{\dagger}_\beta(x)]\,, \tag{2-7}$$

and $x \equiv (\underset{\sim}{x}, \tau)$. For very large y, we use the asymptotic form of $D_{\alpha\beta}$:

$$\begin{aligned} & D_{\alpha\beta}(y - x) \\ & \approx \delta_{\alpha\beta} \int \frac{d\omega}{2\pi} \; \frac{1}{4\pi y} \; e^{-i\omega(t-y) - i\underset{\sim}{k}\cdot\underset{\sim}{x} + i\omega\tau} \\ & \times \theta(t - \tau)\,, \end{aligned} \tag{2-8}$$

where $\underset{\sim}{k} \equiv \omega\hat{\underset{\sim}{y}}$, and α, β are restricted to vector components perpendicular to $\underset{\sim}{k}$.

Substituting (2-8) in (2-5,6), we obtain, for large t_1, t_2,

$$\begin{aligned} \langle A^{\dagger}_\alpha(y_1)\, A_\beta(y_2)\rangle &= \frac{|g|^2}{(4\pi)^2\, y_1 y_2} \int \frac{d\omega_1}{2\pi} \; \frac{d\omega_2}{2\pi} \; e^{i\omega_1(t_1 - y_1) - i\omega_2(t_2 - y_2)} \\ &\times \int d^4x_1 \, d^4x_2 \; e^{-ik_1\cdot x_1 + ik_2\cdot x_2} \, \langle j^{\dagger}_\alpha(x_1)\, j_\beta(x_2)\rangle\,, \end{aligned} \tag{2-9}$$

$$\langle \left(A_\alpha^\dagger(y_1)\, A_\beta^\dagger(y_2)\right)_- \left(A_\beta(y_2)\, A_\alpha(y_1)\right)_+ \rangle$$

$$= \left[|g|^2/(4\pi)^2 y_1 y_2\right]^2 \int \frac{d\omega_1}{2\pi} \frac{d\omega_2}{2\pi} \frac{d\omega'_1}{2\pi} \frac{d\omega'_2}{2\pi}$$

$$\times\ e^{-i(\omega'_2-\omega_2)(t_2-y_2)-i(\omega'_1-\omega_1)(t_1-y_1)}$$

$$\times \int d^4x_1\, d^4x_2\, d^4x'_1\, d^4x'_2\, e^{-ik_1\cdot x_1 - ik_2\cdot x_2 + ik'_1\cdot x'_1 + ik'_2\cdot x'_2}$$

$$\times \langle \left(j_\alpha^\dagger(x_1)\, j_\beta^\dagger(x_2)\right)_- \left(j_\beta(x'_2)\, j_\alpha(x'_1)\right)_+ \rangle \ , \qquad (2\text{-}10)$$

where $k\cdot x \equiv \omega\tau - \underset{\sim}{k}\cdot\underset{\sim}{x}$. We assume that $\hat{\hat{y}}_1 \approx \hat{y}_2$ so that $\underset{\sim}{k}_1$, $\underset{\sim}{k}_2$, $\underset{\sim}{k}'_1$, $\underset{\sim}{k}'_2$ all point in the same direction (see Figure 1).

Equations (2-9, 10) express the photon correlation functions in terms of the Fourier transforms of the current correlation functions, which will be investigated within the framework of a simple model under various assumptions.

III. THE SOURCE MODEL

A. Assumptions

We like the model to be described in as few parameters as possible and still retain some features of a physically realistic source. We now describe our model.

(a) The source is a stationary, uniform, and isotropic gas of colliding atoms. We are concerned only with the two levels (each may be degenerate) which produce the spectral line of interest.

(b) To avoid describing specific methods of excitation we let the source be in thermal equilibrium. The parameters, temperature and chemical potential, determine the excitation level as well as the density, the pressure, etc., of the atoms. In other words, we replace the detailed external excitation mechanism by a reservoir so that the energy lost in radiation is always gained back from the reservoir.

In order to maintain the population difference so that photons are generated at a constant rate, the interaction between the reservoir and the atoms must be strong enough. However, a stronger coupling implies more perturbation on the atom amplitudes and hence more fluctuation in the electromagnetic field outside. Therefore, we have to assume that the fluctuations due to the collisions included in the model are the dominating ones and that the rate of radiation loss is small.

The simplifying feature of the thermal equilibrium assumption is that all the statistical properties of the model are summarized by the grand canonical ensemble, which can be handled by the method of the temperature Green's function to be described later.

(c) The source is small and has a transparent boundary. The spectral line width Γ is assumed to be much less than Γ_c. This implies that the emitted photon wave packet, which has the size of $1/\Gamma$, is much larger than the size of the source.

(d) Let E'_0 be the center of the spectral line. We shall restrict the discussion to photon frequencies well within the range Γ_c near E'_0, i.e.,

$$|\omega - E'_0| \ll \Gamma_c \approx 1/L .$$

Since $\Gamma \ll \Gamma_c$, this is not a severe restriction. This allows us to regard the vectors $\underset{\sim}{k}_1$, $\underset{\sim}{k}_2$, $\underset{\sim}{k}'_1$, $\underset{\sim}{k}'_2$ appearing in (2-9) and (2-10) as constant vectors equal to $\underset{\sim}{k} = E'_0 \hat{y}$, since $\omega\hat{y}\cdot\underset{\sim}{x} = (\omega - E'_0)\hat{y} \cdot \underset{\sim}{x} + E'_0 \hat{y} \cdot \underset{\sim}{x} \approx E'_0 \hat{y} \cdot \underset{\sim}{x}$.

The restrictions (c) and (d) simplify the mathematical treatment of the intensity correlation considerably. They are not necessary for our discussion of the amplitude correlation.

(e) The density of the atoms is low, i.e., the occupation number per state is much less than one. We shall ignore powers of occupation numbers higher than the first.

(f) The atoms collide via central force so that the <u>total</u> spin is conserved in collision processes.

(g) Excitations by collisions will not be included in the Hamiltonian, although we shall include collisions involving the transfer of internal energy from one atom to another. Therefore, the excited atoms are all

generated by the thermal reservoir. In view of the adiabatic principle, the excitation of electronic levels by collisions is not probable until the kinetic energy of the atoms approaches the threshold energy times the atom-electron mass ratio.[5] We restrict our discussion to temperatures low enough to involve a gas of atoms instead of a plasma.

(h) Surface phenomena are ignored. The source is much larger than the atom mean free path so that the source medium may be regarded as infinite when calculating the current correlation functions.

Under the above assumptions, the expressions for the amplitude correlation function (2-9) reduces to

$$\langle A_\alpha^\dagger(y_1)\, A_\beta(y_2)\rangle = \delta_{\alpha\beta}|g|^2\, V\,[(4\pi)^2\, y_1 y_2]^{-1} \times \int \frac{d\omega}{2\pi}\; e^{-i\omega(t_2-y_2-t_1+y_1)}\; S(\omega)\,, \tag{3-1}$$

where

$$S(\omega) \equiv \int dt\; e^{i\omega t}\, \langle j_\alpha^\dagger(\underset{\sim}{k})\, j_\alpha(\underset{\sim}{k};t)\rangle\,. \tag{3-2}$$

Under the assumptions (c) and (d), we obtain from (2-10), after some algebra,

$$\langle \left(A_\alpha^\dagger(y_1)\, A_\beta^\dagger(y_2)\right)_- \left(A_\beta(y_2)\, A_\alpha(y_1)\right)_+\rangle = [\,|g|^2\, V/(4\pi)^2\, y_1 y_2]^2 \int \frac{d\nu}{2\pi}\; e^{-i\nu(t_2-y_2-t_1+y_1)}\; J(\alpha\beta,\nu)\,, \tag{3-3}$$

where

$$J(\alpha\,\beta,\nu)$$

$$\equiv \int dt\; e^{i\nu t}\; \langle \left(j_\alpha^\dagger(\underset{\sim}{k})\; j_\beta^\dagger(\underset{\sim}{k},t)\right)_- \left(j_\beta(\underset{\sim}{k},t)\; j_\alpha(\underset{\sim}{k})\right)_+ \rangle\;, \tag{3-4}$$

The operator $j_\mu(\underset{\sim}{k},t)$ in (3-2,4) is defined by

$$j_\mu(\underset{\sim}{k},t) \equiv V^{-\frac{1}{2}} \int d^3x\; e^{-i\underset{\sim}{k}\cdot\underset{\sim}{x}}\; j_\mu(\underset{\sim}{x},t)\;, \tag{3-5}$$

where V is the volume of the source. $S(\omega)$ is independent of α. $S(\omega)$ shall be called the power spectrum. The averages are taken over a grand canonical ensemble of temperature $1/\beta$ and chemical potential μ.

B. Notation and Further Description

1. Atoms

Let the two atomic levels of interest have angular momenta j_1, j_2 and internal energies 0, E_0 (see Figure 2). The two levels are $(2j_{1,2} + 1)$-fold degenerate, respectively. The atoms are described by a $(2j_1 + 1 + 2j_2 + 1)$--component annihilation operator:

$$\begin{pmatrix} b(\underset{\sim}{p}) \\ c(\underset{\sim}{p}) \end{pmatrix},$$

where b annihilates an atom in the lower level and c annihilates one in the upper level:

$$b(\underset{\sim}{p}) = \begin{pmatrix} b_{j_1}(\underset{\sim}{p}) \\ \vdots \\ b_{m_1}(\underset{\sim}{p}) \\ \vdots \\ b_{-j_1}(\underset{\sim}{p}) \end{pmatrix} , \qquad c(p) = \begin{pmatrix} c_{j_2}(\underset{\sim}{p}) \\ \vdots \\ c_{m_2}(\underset{\sim}{p}) \\ \vdots \\ c_{-j_2}(\underset{\sim}{p}) \end{pmatrix} . \qquad (3\text{-}6)$$

$\underset{\sim}{p}$ is the momentum of the atom. The z-axis is always along $\underset{\sim}{k}$, which points from the source to the observer. Without loss of generality, b,c are regarded as boson operators.

2. The Current Operator

The current operator is a vector coupled to the photon. It must change the state of an atom from the upper to the lower level in order to create a photon of interest. The most general vector one can construct out of c and $b^\dagger$ is of the form

$$j_\mu(\underset{\sim}{k}) = V^{-\frac{1}{2}} \sum_{m_1 m_2 \underset{\sim}{p}} b^\dagger_{m_1}(\underset{\sim}{p})\, c_{m_2}(\underset{\sim}{p} + \underset{\sim}{k})\, \langle j_2 m_2 | j_1 m_1 1 \mu \rangle . \qquad (3\text{-}7)$$

$\langle j_2 m_2 | j_1 m_1 1 \mu \rangle$ are the usual Wigner Coefficients; $\mu = \pm 1$. We shall represent an atom in the lower (upper) level by a thin (thick) line, and use the label b or 1 (c or 2) to denote the lower (upper) level.

3. Collision Terms

Four kinds of collision terms are included (see Figs. 4 a,b,c,d):

(a) $A^b + B^b \to A^b + B^b$, scattering of atoms in the lower level,

(b) $A^c + B^c \to A^c + B^c$, scattering of those in the upper level,

(c) $A^b + B^c \rightarrow A^b + B^c$, scattering of an atom in the lower level by one in the upper level, and

(d) $A^b + B^c \rightarrow A^c + B^b$, which is the same as (c) except that the excitation is transferred from B to A .

The separation between (c) and (d) is artificial (but convenient) since all atoms are identical.

Process (a) gives an interaction term:

$$\sum_{\text{all } p\text{'s and } m\text{'s}} V^{bb}_{m'm''mm''} \left(\underset{\sim}{p} - \underset{\sim}{p}'\right) b^{\dagger}_{m'}(\underset{\sim}{p}')\, b^{\dagger}_{m'''}(\underset{\sim}{p} + \underset{\sim}{p}'' - \underset{\sim}{p}') \times b_{m}(\underset{\sim}{p})\, b_{m''}(\underset{\sim}{p}'') \quad . \tag{3-8}$$

Since we assume that all forces are central forces, the total spin is conserved. It is convenient to expand the potential V^{bb} into a sum of terms each one of which corresponds to a definite "spin transfer" analogous to the momentum transfer $\underset{\sim}{p} - \underset{\sim}{p}'$:

$$V^{bb}_{m'm''mm''} = \sum_{J,M} V^{bb}_{J} (2J+1)^{\frac{1}{2}} \langle j_1 m' \; JM | j_1 m \rangle \times \langle j_1 m'' \; JM | j_1 m''' \rangle \quad . \tag{3-9}$$

The amplitude of transfering angular moment (J,M) from the particle on the left in Fig. 4a to that on the right is then proportional to V^{bb}_{J} . In exactly the same manner, we can write a term like (3-8) for (b), (c), and (d). We also define the spin transfer potentials

V_J^{cc} , V_J^{bc} , $\tilde{V}_J^{bc}$ for (b), (c), and (d), respectively, in exactly the same way as we defined V_J^{bb} :

$$V^{cc}_{m'_2 m''_2 m_2 m''_2} = \sum_{J,M} V_J^{cc} (2J+1)^{\frac{1}{2}} \langle j_2 m_2 | j_2 m' \, JM \rangle \times \langle j_2 m'''_2 | j_2 m''_2 \, JM \rangle \ ,$$

$$V^{bc}_{m'_2 m''_1 m_2 m''_1} = \sum_{J,M} V_J^{bc} (2J+1)^{\frac{1}{2}} \times \langle j_2 m_2 | j_2 m'_2 \, JM \rangle \langle j_1 m'''_1 | j_1 m''_1 \, JM \rangle \ ,$$

$$\tilde{V}^{bc}_{m'_2 m'''_1 m_1 m''_2} = \sum_{J,M} \tilde{V}_J^{bc} (2J+1)^{\frac{1}{2}} \times \langle j_2 m_2 | j_1 m'_1 \, JM \rangle \langle j_2 m'''_2 | j_1 m''_1 \, JM \rangle \ . \qquad (3\text{-}10)$$

4. Reabsorption of Photons by Atoms

Before a photon reaches the surface, there is a probability that it will be reabsorbed by an atom. The reabsorption rate is, as a function of frequency ω , directly proportional to the emission rate. Let $\alpha(\omega)$ be the absorption rate and Γ_c be the leak rate in the absence of reabsorption. Then the probability for a photon to leak out in the presence of reabsorption is

$$\frac{\Gamma_c}{\Gamma_c + \alpha(\omega)} \ . \qquad (3\text{-}11)$$

Therefore, the rate of photon output is proportional to

$$\alpha(\omega) \Big/ \left(1 + \frac{\alpha(\omega)}{\Gamma_c}\right) . \qquad (3\text{-}12)$$

The larger Γ_c is, the less will be the effect of the reabsorption on the output. In the limit when $\alpha(\omega) \gg \Gamma_c$, (3-12) simply gives Γ_c. In other words, the source behaves like a box of free photons in thermal equilibrium, as will be seen in more detail later.

We may also look upon the process of emission and the subsequent reabsorption as an atom-atom scattering process with internal energy transfer by the exchange of a virtual photon (see Fig. 4e) similar to that shown in Fig. 4d, except that the emission and the absorption are not simultaneous. It is important to notice that the time delay is limited by $1/\Gamma_c$, after which the photon will be outside the source.

We like to emphasize that this is a much more correct way to look at the reabsorption process, one of the many processes in which the internal energy of one atom is transferred to another atom. The sole fact that a photon is carrying the energy across has no significance. The reason for giving special attention to photon reabsorption is that such an energy exchange process is strong and of long range.

The propagation of an exchanged photon will be treated phenomenologically as a damped cavity mode coupled to the atoms.

C. Method of Calculation

The equations (3-1), (3-2), (3-3), (3-4), and (3-5) form the basis of our calculation. The task is to calculate the current

correlation functions (3-2), and (3-4), for an interacting many body system. The thermal equilibrium assumption enables us to use the temperature Green's function method.[6] In the next chapter, we shall review some basic ideas of the method and derive some formulas needed later.

IV. TEMPERATURE GREEN'S FUNCTIONS

A. General Procedure of the Temperature Green's Function Method

The motivation of the method is the following. Often we like to calculate a correlation function of the type:

$$CF(t_1, t_2, \ldots t_n) = \mathrm{Tr}\{\rho\, A(t_1)\, B(t_2) \ldots C(t_n)\}\ , \qquad (4\text{-}1)$$

where

$$A(t_1) = e^{iHt_1}\, A\, e^{-iHt_1}\ , \text{ etc.},$$

and

$$\rho = Z^{-1}\, e^{-\beta H}\ ,\ Z = \mathrm{Tr}\, e^{-\beta H}\ .$$

From now on H is the Hamiltonian minus μN (or $\sum_i \mu_i N_i$ if more than one species of particles have non-zero chemical potential). This means that the energy of a particle is measured from its chemical potential. Since only energy differences usually appear in the results, this change of the energy scale has no effect. It is generally very difficult to construct a perturbation expansion for CF. On the other hand, the temperature Green's function:

$$TGF(\tau_1, \tau_2 \cdots \tau_n) = \mathrm{Tr}\{\rho\, T(\hat{A}(\tau_1)\hat{B}(\tau_2)\cdots\hat{C}(\tau_n))\}\ , \qquad (4\text{-}2)$$

where $\hat{A}(\tau_1) = e^{\tau_1 H}\, A\, e^{-\tau_1 H}$, etc., $0 \leqslant \tau_i \leqslant \beta$ and T orders the operators so that larger τ appears to the left, is relatively easy to obtain by perturbation expansion.

Since one is not interested in TGF itself but rather in CF, one then hopes to find a connection between CF and TGF. This connection turns out to be quite simple for $n = 2$, (n = number of operators appearing in (4-1) or (4-2) in addition to ρ). It can always be derived and it will be derived for $n = 2,3$. (See Section B of this chapter and Chapter VII.) Therefore CF can be obtained once TGF is known.

The perturbation expansion for TGF[6] is just the Feynman-Dyson expansion in the usual field theory with imaginary time running between 0 and $-i\beta$ and with the vacuum expectation replaced by averaging over the unperturbed ensemble

$$\rho_0 = e^{-\beta H_0} / \mathrm{Tr}\, e^{-\beta H_0} :$$

$$\mathrm{TGF}(\tau_1, \tau_2, \cdots \tau_n) = \sum_{m=0}^{\infty} \frac{(-)^m}{m!} \int_0^{\beta} d\tau'_1\, d\tau'_2 \cdots d\tau'_m$$

$$\times \mathrm{Tr}\{\rho_0\, T(\hat{A}_I(\tau_1)\, \hat{B}_I(\tau_2) \cdots \hat{C}_I(\tau_n)\, \hat{H}_I(\tau'_1) \cdots \hat{H}_I(\tau'_m))\} \qquad (4\text{-}3)$$

$$\times \Big[\sum_{m=0}^{\infty} \frac{(-)^m}{m!} \int_0^{\beta} d\tau'_1 \cdots d\tau'_m\, \mathrm{Tr}\{\rho_0\, T(\hat{H}_I(\tau'_1) \cdots \hat{H}_I(\tau'_m))\}\Big]^{-1} ,$$

where $\hat{A}_I(\tau) = e^{\tau H_0} A\, e^{-\tau H_0}$, etc. ; H_0 is the unperturbed Hamiltonian minus μN .

Every term in the expansion is the average of a product of creation and annihilation operators over the unperturbed ensemble. To construct a diagrammatic representation of the terms, one needs a Wick's

Theorem to contract the average of a product to a sum of products of averages of pairs. This is indeed possible for a large system. The derivation of general diagram rules are well-known[6] and will not be repeated here. Rules for calculation with our model will be specified when needed.

The general procedure of calculating CF by the temperature Green's Function technique may be summarized as follows: First, derive the connection between the CF of interest and some TGF . Second, calculate TGF by diagram technique. Then finally calculate CF from TGF .

B. Temperature Greens' Functions of Two Time Arguments

In this section, we derive the connection between CF and TGF defined in (4-1,2) with $n = 2$, i.e., for

$$CF(t_1, t_2) = Tr\{\rho\, A(t_1)\, B(t_2)\} , \tag{4-4}$$

$$TGF(\tau_1, \tau_2) = Tr\{\rho\, T(\hat{A}(\tau_1)\, \hat{B}(\tau_2))\} . \tag{4-5}$$

Without loss of generality, we exclude the possibility that A,B are <u>single</u> fermion operators. Clearly, CF is a function of $t_2 - t_1 \equiv t$ only, and TGF is a function of $\tau_2 - \tau_1 \equiv \tau$ only. Let $CF(\omega)$ be defined by

$$CF(\omega) = \int dt\, e^{i\omega t}\, CF(0,t) . \tag{4-6}$$

Expanding (4-5,6) in terms of matrix elements between eigenstates of H, we find

$$CF(\omega) = Z^{-1} \sum_{a,b} e^{-\beta E_a} A_{ab} B_{ba} 2\pi \delta(\omega + E_{ba}) , \qquad (4\text{-}7)$$

where

$$E_{ba} = E_b - E_a ,$$

and

$$TGF(0,\tau) = Z^{-1} \sum_{a,b} e^{-\beta E_a} A_{ab} B_{ba} e^{E_{ba}\tau} \qquad (4\text{-}8)$$

if $\tau < 0$, and

$$TGF(0,\tau) = Z^{-1} \sum_{a,b} e^{-\beta E_b} A_{ab} B_{ba} e^{E_{ba}\tau} \qquad (4\text{-}9)$$

if $\tau > 0$.

For $\tau < 0$, $\tau + \beta > 0$, (4-8,9) imply that

$$TGF(0,\tau) = TGF(0,\tau + \beta) .$$

Therefore, $TGF(0,\tau)$ may be represented by the Fourier series

$$TGF(0,\tau) = \frac{1}{\beta} \sum_{\omega_n} e^{-\omega_n \tau} TGF(\omega_n) ,$$

where

$$TGF(\omega_n) = \int_0^\beta d\tau\, e^{\omega_n \tau}\, TGF(0,\tau)\,, \tag{4-10}$$

and

$$\omega_n = (2\pi i/\beta) \cdot \text{integer}.$$

From (4-8,9,10) we obtain the "spectral representation"

$$TGF(\omega_n) = \int_{-\infty}^{\infty} \frac{d\omega'}{2\pi}\, \frac{\rho(\omega')}{\omega' - \omega_n}\,, \tag{4-11}$$

where the "spectral function" $\rho(\omega')$ is defined by

$$\rho(\omega') = -\sum_{a,b} A_{ab} B_{ba} \left(e^{-\beta E_a} - e^{-\beta E_b}\right) \times 2\pi\, \delta(\omega' + E_{ba})\,. \tag{4-12}$$

Comparing (4-12) and (4-7), we see that

$$\rho(\omega') = \int dt\, e^{i\omega t} \langle [B(t),A] \rangle\,, \tag{4-13}$$

and

$$\int \frac{d\omega'}{2\pi}\, \rho(\omega') = \langle [B,A] \rangle\,. \tag{4-14}$$

Therefore, the integral in (4-11) is well-defined if $\langle [B(t),A] \rangle$ is well-defined. $TGF(\omega_n)$ can be continued into the ω-plane by replacing ω_n in (4-11) by the complex variable ω. $TGF(\omega)$ is then an analytic function in the ω-plane cut along the real axis. The analytic continuation

is unique if the function does not blow up as fast as $e^{\beta|\omega|/2}$ according to the Carlson's Theorem familiar in Regge Pole Theory.[7] TGF(ω) approaches $1/\omega$ as $|\omega| \to \infty$, according to (4-11). $\rho(\omega)$ and CF(ω) can now be found from the discontinuity of TGF(ω) across the real axis:

$$\rho(\omega) = -i\,[\mathrm{TGF}(\omega + i\eta) - \mathrm{TGF}(\omega - i\eta)]\,,$$
$$\mathrm{CF}(\omega) = \rho(\omega)\,[e^{\beta\omega} - 1]^{-1}\,. \qquad (4\text{-}15)$$

The symbol η will always denote an infinitesimal positive number. Finally, $\mathrm{CF}(t_1, t_2)$ is obtained from CF(ω) by Fourier transform. The connection between CF and TGF is now clear and will be applied in the next chapter to find the current correlation function $\langle j_\alpha^\dagger(\underset{\sim}{k}) j_\alpha(\underset{\sim}{k}, t)\rangle$.

Before proceeding, let us consider the trivial but instructive case where $A = B = 1$. Then, obviously, by (4-4,5,6,10,13),

$$\mathrm{CF}(t_1, t_2) = \mathrm{TGF}(\tau_1, \tau_2) = 1\,,$$
$$\mathrm{CF}(\omega) = 2\pi\,\delta(\omega)\,,$$
$$\mathrm{TGF}(\omega_n) = \beta\,\delta_{\omega_n, 0}\,,$$
$$\rho(\omega) = 0\,. \qquad (4\text{-}16)$$

The fact that $\rho(\omega) = 0$ does not imply that $CF(\omega) = 0$. The factor $(e^{\beta\omega} - 1)^{-1}$ in (4-15) becomes infinite at $\omega = 0$. One must handle the Kronecker delta properly in order to obtain consistent results. Let us use the representation

$$\delta^K(\omega_n) = \frac{1}{\beta} \int \frac{d\omega'}{2\pi} \frac{e^{\beta\omega'} - 1}{\omega' - \omega_n} [2\pi\, \delta(\omega')] \qquad (4\text{-}17)$$

for $\delta_{\omega_n, 0}$. The δ-function in (4-17) is regarded as sharply peaked but the limit of infinite sharpness is taken only at the end of a calculation. Replacing the discrete ω_n by the complex variable ω, we obtain $\delta^K(\omega)$, the analytic continuation of the Kronecker delta. $\delta^K(\omega)$ is discontinuous across $\mathrm{Im}\ \omega = 0$, and the discontinuity is

$$\delta^K(\omega + i\eta) - \delta^K(\omega - i\eta) = \frac{2\pi i}{\beta} \delta(\omega) (e^{\beta\omega} - 1) . \qquad (4\text{-}17')$$

Using this for $\rho(\omega)$, we see that (4-15) gives the correct $CF(\omega)$.

C. Temperature Green's Functions with Arbitrary Number of Times

The results of the preceding section suggest that the analytically continued Fourier coefficient is important. It is quite clear that the temperature Green's functions with more than two times can be expanded in multiple Fourier series and the Fourier coefficients will be well defined. In this section we shall derive some trivial but useful results concerning the analytic and asymptotic behavior of the Fourier coefficients of a temperature Green's function of an arbitrary number of "time" arguments.

1. Asymptotic Behavior of the Fourier Coefficient

Consider the TGF defined by (4-2). Without losing much generality, we assume that none of the operators A, B,....C is a fermion operator. TGF is a function of the differences among $\tau_1, \tau_2, \cdots, \tau_n$. There are n-1 independent differences. Let $t_1, t_2, \cdots, t_{n-1}$ be a set of n-1 independent differences. We then expand TGF in an (n-1)-dimensional Fourier series. The Fourier coefficient can be shown to be

$$\begin{aligned} &\mathrm{TGF}(\omega_1, \omega_2, \cdots \omega_{n-1}) \\ &= \beta^{-n+1} \int_0^\beta dt_1 \cdots dt_{n-1} \; e^{\omega_1 t_1 + \cdots + \omega_{n-1} t_{n-1}} \qquad (4\text{-}18) \\ &\times \mathrm{TGF}(t_1, t_2, \cdots t_{n-1}) \; , \end{aligned}$$

where

$$\omega_m = (\text{integer}) \times 2\pi \, i/\beta \; ,$$

$m = 1, 2, \cdots, n-1$.

Equation (4-18) is an integral over a finite range. Obviously, $\mathrm{TGF}(\omega_1, \cdots \omega_{n-1})$ is always finite (of course, $\mathrm{TGF}(t_1, \cdots, t_{n-1})$ is assumed to be finite.). As any one of the ω's tends to infinity, we expect the Fourier coefficient to vanish. To see how it vanishes, let us hold $\omega_2, \cdots \omega_{n-1}$ fixed and integrate t_1 by parts:

$$TGF(\omega_1, \omega_2, \cdots, \omega_{n-1})$$

$$= (\beta\omega_1)^{-1} [TGF(\beta, \omega_2, \cdots, \omega_{n-1})$$

$$- TGF(0, \omega_2, \cdots, \omega_{n-1})]$$

$$- (\beta\omega_1)^{-1} \int_0^\beta dt_1 \; e^{\omega_1 t_1} \; \frac{d}{dt_1} \; TGF(t_1, \omega_2 \cdots) \; . \qquad (4\text{-}19)$$

TGF can only have a finite number of jumps as a function of t_1 due to the change of ordering of the operators. The integral in (4-19) is therefore finite. We conclude

$$\lim_{\omega_m \to \infty} \; TGF(\omega_1, \cdots \omega_m, \cdots \omega_{n-1}) \; = \; O(\omega_m^{-1}) \; . \qquad (4\text{-}20)$$

We can arrive at conclusions stronger than (4-20) by arguing in terms of the perturbation expansion, which we assume to converge. Since TGF is just a sum of the products of contractions and ω_m appears only in the energy denominators of the contractions, TGF must vanish like $O(1/\omega_m)$, not only for ω_m along the descrete set on the imaginary axis, but also for ω_m along any line in the complex ω_m-plane.

In view of Carlson's Theorem, the convergence of the perturbation expansion also implies the existence of a unique analytic continuation of the Fourier coefficient, because every term in the expansion can be analytically continued.

One can study the Fourier coefficient by constructing the spectral representation explicitly in terms of the matrix elements of the operators between energy eigenstates of the system. This is done for the case $n = 2$ (Section B of this chapter) and for $n = 3$ (Chapter VII). However, for $n > 3$, explicit constructions are impractical. We procede to show that the essential feature of the analytic structure can be derived through very simple arguments.

2. Cuts for the Analytically Continued Fourier Coefficient

Let us introduce one more frequency variable ω_n:

$$\omega_n \equiv -\omega_1 - \omega_2 - \cdots - \omega_{n-1} \quad . \tag{4-21}$$

We define the frequencies in such a way that

$$\begin{aligned} &TGF(\tau_1, \cdots, \tau_n) \\ &= \beta^{-n+1} \sum_{\omega_1, \cdots \omega_n} \delta_{\omega_1 + \cdots + \omega_n, 0} \; e^{-\omega_1 \tau_1 - \cdots - \omega_n \tau_n} \\ &\times TGF(\omega_1, \cdots \omega_{n-1}, \omega_n) \; . \end{aligned} \tag{4-22}$$

This way, a frequency can be associated with each operator. We represent the analytically continued Fourier coefficient by a diagram (see Fig. 3a). The operators $A, B, \cdots, C$ form n "ends" or "external lines" with energy $\omega_1, \cdots, \omega_n$, respectively. The following physical arguments will clarify the analytic properties of the Fourier coefficient.

In Section B of this chapter, we expanded the one-frequency Fourier coefficient in the matrix elements A_{ab} , B_{bc} . We found that the Fourier coefficient becomes singular when

$$\omega = E_{ab} ,$$
$$A_{ab} \neq 0 , \text{ and } B_{ba} \neq 0 . \qquad (4\text{-}23)$$

i.e., when a resonance between the two energy eigenstates a and b is possible. To make our later arguments intuitively clear, let us call such a resonance between two eigenstates of the system an "elementary excitation" of the system, or a "particle" in the medium. It has energy E_{ab} and symmetry properties determined by the states a and b . The ends A,B represent the external disturbance. The rule (4-23) is simply the condition for energy and symmetry conservation. Thus, if an elementary excitation can exist between B and A (see Fig. 3b) with all conservation laws satisfied, the Fourier coefficient is singular.

The generalization is clear: The Fourier coefficient is singular if an elementary excitation can be created and destroyed by the external lines with all conservation laws satisfied.

For a large system, there are elementary excitations available with all energies and symmetries so that the Fourier coefficient is singular whenever a partial sum of the external line energies becomes real. This rule is very useful. For example, consider the case of four external lines with energies ω_1, ω_2, ω_3 , and $\omega_4 \equiv -\omega_1 - \omega_2 - \omega_3$.

Figure 3c shows how the "elementary excitations" are created and destroyed by the external lines. By our rule, the Fourier coefficient is singular when one or more of the following is real:

$$\omega_1,\ \omega_2,\ \omega_3,\ \omega_4\ ,$$

$$\omega_1 + \omega_2,\ \omega_1 + \omega_3,\ \omega_1 + \omega_4\ ,$$

i.e., there are seven cuts (or rather "cut planes") given by

$$\mathrm{Im}\ \omega_1 = 0\ ,\ \ldots\ldots\ldots\ldots\ ,\ \mathrm{Im}(\omega_1 + \omega_4) = 0$$

in the space of three complex variables.

V. THE POWER SPECTRUM

A. The Green's Function

The power spectrum $S(\omega)$, which we now proceed to calculate, is defined by (3-2):

$$S(\omega) = \int dt\, e^{i\omega t} \langle j_\mu^+(\underset{\sim}{k})\, j_\mu(\underset{\sim}{k},t)\rangle \,. \tag{5-1}$$

$S(\omega)$ is independent of μ, and μ is not summed. It is related to the temperature Green's function

$$\mathcal{G}(\tau) = \langle T[j_\alpha^\dagger(\underset{\sim}{k})\, \hat{j}_\alpha(\underset{\sim}{k},\tau)]\rangle \tag{5-2}$$

through (4-15). If we substitute $j_\alpha^\dagger(\underset{\sim}{k})$ for A and $j_\alpha(\underset{\sim}{k})$ for B in Section B of last chapter, then CF = S and TGF = $\mathcal{G}$. The spectral function defined by (4-12) is now real since $A_{ab}\, B_{ba} = |j_{\alpha\, ba}|^2$. Equation (4-15) now reads:

$$\begin{aligned} S(\omega) &= -i[\mathcal{G}(\omega + i\eta) - \mathcal{G}(\omega - i\eta)]/(e^{\beta\omega} - 1) \\ &= 2\, \mathrm{Im}\,\mathcal{G}(\omega + i\eta)/(e^{\beta\omega} - 1) \,. \end{aligned} \tag{5-3}$$

The next step is to find the Fourier coefficient $\mathcal{G}(\omega_n)$ and its analytic continuation, which will be referred to as the "Green's function."

B. Representation by Diagrams

Let a thick line represent the contraction of an annihilation operator and a creation operator for an atom in the upper level, and a thin line represent that for an atom in the lower level. Arrows point to the annihilation. These are the atom propagators. The interaction potentials (defined in Section III.B, see also Fig. 4) will be represented by dashed lines. The virtual photon is represented by a wavy line.

The rules for calculating a given diagram are the following.

a. Vertices. For every dashed line, we write (-1) times the appropriate potential labeled by spin indices of the atom lines connected to the dashed line.

b. Virtual Photons. The scattering by the exchange of a virtual photon cannot be described by a potential. We use the propagator of a damped traveling cavity mode to describe the virtual photon. We shall only need to consider the mode with momentum $\underset{\sim}{k}$, energy ω_n and spin $\mu = \pm 1$, for which we write

$$- D(\omega_n, \underset{\sim}{k}) = - |g|^2 (2k)^{-1} [\omega_n - k - \Sigma_c(\omega_n, \underset{\sim}{k})] , \qquad (5\text{-}4)$$

where we have included in D the photon-current coupling constant g. $\Sigma_c(\omega_n, \underset{\sim}{k})$ is the self energy of the virtual photon. When ω_n is continued to real value,

$$\Sigma_c(\omega \pm i\eta, \underset{\sim}{k}) \approx \mp i \Gamma_c , \qquad (5\text{-}4')$$

where Γ_c is the phenomenological cavity width introduced before.

c. Atom Propagators. It is convenient to put in the self energy at the beginning. Translation and rotation symmetries plus the assumption of total spin conservation (central forces) allow us to write a factor

$$- G_+(\epsilon_n, \underset{\sim}{p}) = - [\epsilon_n - \epsilon_{\underset{\sim}{p}} - E_0 - \Sigma_+(\epsilon_n, \underset{\sim}{p})]^{-1} \qquad (5\text{-}5)$$

independent of spin orientation for every thick solid line labeled by the energy ϵ_n, spin m, and momentum $\underset{\sim}{p}$, where $\epsilon_{\underset{\sim}{p}}$ is the single atom kinetic energy

$$\epsilon_{\underset{\sim}{p}} = \frac{p^2}{2m} - \mu ,$$

and $\Sigma_+(\epsilon_n, \underset{\sim}{p})$ is the self energy of the upper level atom.

Similarly, for every thin line, we have a factor

$$- G_-(\epsilon_n, \underset{\sim}{p}) = - [\epsilon_n - \epsilon_{\underset{\sim}{p}} - \Sigma_-(\epsilon_n, \underset{\sim}{p})]^{-1} \quad . \qquad (5\text{-}6)$$

$\Sigma_{\pm}$ will be calculated later.

Notice that the single particle kinetic energy is measured from the chemical potential μ.

d. Sums. We then sum and integrate over every energy ϵ_n, spin m, and momentum $\underset{\sim}{p}$ which are not fixed by the energy, spin, and momentum conservation:

$$\prod_i \frac{1}{\beta} \sum_{\epsilon_n} \sum_{m_i} V \int \frac{d^3 p_i}{(2\pi)^3} (\cdots) \quad .$$

The Green's function $\mathcal{G}(\omega_n)$ is the sum of all diagrams with $j_\mu^\dagger(\underset{\sim}{k})$ and $j_\mu(\underset{\sim}{k})$ at the ends (see Fig. 5), which may be broken into terms shown in Fig. 6. $\mathcal{F}$ is the sum of all diagrams with four appropriate corners for hooking up the legs. $\mathcal{F}$ must not include any "intermediate state" with only one thick line up and one thin line down. Fig. 6 suggests the following procedure of summing the diagrams. First, we open up the upper ends of all the diagrams in Fig. 6, and we then have an equation for the vertex function K shown in Fig. 7. We next approximate $\mathcal{F}$ by a few simple diagrams and solve the equation for K. Finally we close the open ends to obtain $\mathcal{G}(\omega_n)$. Before we carry out these steps, we first show how to close the ends of the vertex function K to obtain $\mathcal{G}$.

C. Connection between $\mathcal{G}$ and the Vertex Function K

The vertex function $K_{m_2 m_1 \mu}(\epsilon_n, \omega_n, \underset{\sim}{p})$ has three ends, $b^\dagger_{m_1}(\underset{\sim}{p})$, $c_{m_2}(\underset{\sim}{p} + \underset{\sim}{k})$, and $j^\dagger_\mu(\underset{\sim}{k})$. The assumption of total spin conservation implies that

$$K_{m_2 m_1 \mu}(\epsilon_n, \omega_n, \underset{\sim}{p}) = \langle j_2 m_2 | j_1 m_1 1 \mu \rangle \, K(\epsilon_n, \omega_n, \underset{\sim}{p}) \, . \tag{5-7}$$

$K(\epsilon_n, \omega_n, \underset{\sim}{p})$ is a scalar function. The label $\underset{\sim}{k}$ is suppressed. $\mathcal{G}(\omega_n)$ is obtained from K by summing over the intermediate energy, spin and momentum after closing the open ends:

$$\mathcal{S}(\omega_n) = \sum_{m_1,m_2} \langle j_1 m_1 1\mu | j_2 m_2 \rangle$$

$$\times \frac{1}{\beta} \sum_{\epsilon_n} \int \frac{d^3p}{(2\pi)^3} K_{m_2 m_1 \mu}(\epsilon_n, \omega_n, \underset{\sim}{p}) e^{\eta\epsilon_n} \qquad (5\text{-}8)$$

where $\eta = 0+$ is to insure that $b^\dagger$ stands to the left of c. The Wigner coefficient in (5-8) comes from the definition of $j_\mu(\underset{\sim}{k})$ (see Eq. (3-7)). Since

$$\sum_{m_1,m_2} \langle j_1 m_1 JM | j_2 m_2 \rangle \langle j_1 m_1 J'M' | j_2 m_2 \rangle$$

$$= \delta_{JJ'} \delta_{MM'} (2j_2 + 1)/(2J + 1) , \qquad (5\text{-}9)$$

we have the simple equation

$$\mathcal{S}(\omega_n) = \frac{1}{3}(2j_2 + 1) \frac{1}{\beta} \sum_{\epsilon_n} \int \frac{d^3p}{(2\pi)^3} K(\epsilon_n, \omega_n, \underset{\sim}{p}) e^{\eta\epsilon_n} . \qquad (5\text{-}10)$$

What we are interested in is $\mathrm{Im}\, \mathcal{S}(\omega + i\eta)$ (see Eq. (5-3)). The sum over ϵ_n in (5-10) must be performed before the analytic continuation in ω. To evaluate the sum, we need to know the site of the cuts of $K(\epsilon, \omega_n)$ (as a function of complex ϵ). The analytic structure of a general three end temperature Green's Function is worked out in Chapter VII. K is discontinuous when any of the energies ϵ, ω, $\omega + \epsilon$ becomes real (see the discussion at the end of Chapter IV). The cuts along $\mathrm{Im}\, \omega = 0$, $\mathrm{Im}\, \epsilon = 0$, and $\mathrm{Im}(\epsilon + \omega) = 0$ divide the two-complex-variable space into six regions as shown in Fig. 8. Here we are only interested in $\mathrm{Im}\, \omega > 0$.

On the ϵ-plane, $K(\epsilon,\omega_n)$, as a function of ϵ, has cuts along Im $\epsilon = 0$, and Im $\epsilon = -\omega_n$ (see Fig. 9). The standard procedure of doing the sum over ϵ_n is to replace the sum by an integral along the path C (shown in Fig. 9) enclosing the points ϵ_n:

$$\frac{1}{\beta}\sum_{\epsilon_n} \rightarrow \int_C \frac{d\epsilon}{2\pi i}\ \frac{1}{e^{\beta\epsilon}-1}\ . \qquad (5\text{-}11)$$

Then one deforms the contour so that the integrals are just above and below the cuts. The integral along the infinite circle vanishes due to the factor $e^{\eta\epsilon}/(e^{\beta\epsilon}-1)$. Let $K^1(\epsilon,\omega)$, $K^2(\epsilon,\omega)$, and $K^3(\epsilon,\omega)$ be the analytic continuation of $K(\epsilon_n,\omega_n)$ into the regions 1,2,3 (see Figs. 8,9), respectively. Then (5-10) becomes

$$\mathfrak{P}(\omega+i\eta) = \int \frac{d^3p}{(2\pi)^3} \int_{-\infty}^{\infty} \frac{d\epsilon}{2\pi i}\ \frac{1}{e^{\beta\epsilon}-1}\ \left[K^{23}(\epsilon-\omega,\omega,\underset{\sim}{p}) + K^{12}(\epsilon,\omega,\underset{\sim}{p})\right]\ (2j_2+1)/3\ , \qquad (5\text{-}12)$$

where K^{ij} stands for $K^i - K^j$.

D. The Integral Equation for the Vertex Function

In this section we shall write down the integral equation for K represented by the diagrams in Fig. 7, simplify it, and analytically continue it to real energy variables.

The four corner function $\mathfrak{F}_{m_2m_1m'_2m'_1}$ in Figs. 6,7 may, under the central force assumption, be written in the form

$$\mathcal{F}_{m_2 m_1 m'_2 m'_1}(\epsilon_n, \epsilon'_n, \omega_n, \underset{\sim}{p}, \underset{\sim}{p}')$$

$$= \sum_{J,M} \frac{2J+1}{2j_2+1} \mathcal{F}_J(\epsilon_n, \epsilon'_n, \omega_n, \underset{\sim}{p}, \underset{\sim}{p}')$$

$$\times \langle j_1 m_1 \, JM | j_2 m_2 \rangle \langle j_1 m'_1 \, JM | j_2 m'_2 \rangle \quad . \tag{5-13}$$

$\mathcal{F}_J$ can be obtained from $\mathcal{F}_{m_2 m_1 m'_2 m'_1}$ by

$$\mathcal{F}_J = \sum_{m_1 m_2 m'_1 m'_2} \frac{2J+1}{2j_2+1} \mathcal{F}_{m_2 m_1 m'_2 m'_1}$$

$$\times \langle j_1 m_1 \, JM | j_2 m_2 \rangle \langle j_1 m'_1 \, JM | j_2 m'_2 \rangle \quad . \tag{5-14}$$

The equation represented by Fig. 7 is then

$$K(\epsilon_n, \omega_n, \underset{\sim}{p}) = G_+(\epsilon_n + \omega_n, \underset{\sim}{p} + \underset{\sim}{k}) \, G_-(\epsilon_n, \underset{\sim}{p})$$

$$\times \left[1 + \frac{1}{\beta} \sum_{\epsilon'_n} \int \frac{d^3 p'}{(2\pi)^3} \mathcal{F}_1(\epsilon_n, \epsilon'_n, \omega_n, \underset{\sim}{p}, \underset{\sim}{p}') \, K(\epsilon'_n, \omega_n, \underset{\sim}{p}') \, e^{\eta \epsilon'_n} \right] . \tag{5-15}$$

All the Wigner coefficients are factored out. Before doing the ϵ'_n sum in (5-15) we consider the common factor

$$K_0(\epsilon_n, \omega_n, \underset{\sim}{p}_n)$$

$$\equiv G_+(\epsilon_n + \omega_n, \underset{\sim}{p} + \underset{\sim}{k}) \, G_-(\epsilon_n, \underset{\sim}{p}) \tag{5-16}$$

on the right hand side and make some simplifications.

Let the retarded and the advanced propagators $G_{\pm}^{R,A}$ be defined as (see Eqs. (5-5,6))

$$G_{+}^{R,A}(p + k) = G_{+}(\epsilon + \omega \pm i\eta, \underset{\sim}{p} + \underset{\sim}{k})$$

$$= \left[\epsilon - \epsilon_{\underset{\sim}{p}} + \omega - E_0 - \underset{\sim}{p}\cdot\underset{\sim}{k}\, m^{-1} \pm i\eta - \Sigma_{+}^{R,A}(p + k)\right]^{-1}, \quad (5\text{-}17)$$

$$G_{-}^{R,A}(p) = G_{-}(\epsilon \pm i\eta, \underset{\sim}{p})$$

$$= [\epsilon - \epsilon_{p} \pm i\eta - \Sigma_{-}^{R,A}(p)]^{-1}, \quad (5\text{-}18)$$

where p stands for $(\epsilon, \underset{\sim}{p})$ and k for $(\omega, \underset{\sim}{k})$. We have made use of the fact that $k \ll p$ so that

$$\epsilon_{\underset{\sim}{p}+\underset{\sim}{k}} \approx \epsilon_{\underset{\sim}{p}} + \underset{\sim}{k} \cdot \frac{\partial \epsilon_p}{\partial \underset{\sim}{p}} = \epsilon_{\underset{\sim}{p}} + \underset{\sim}{k} \cdot \underset{\sim}{p}/m .$$

The analytic continuation of K_0 in the regions 1,2,3 (see Fig. 8) are

$$K_0^{1} = G_{+}^{R}(p + k)\, G_{-}^{R}(p),$$

$$K_0^{2} = G_{+}^{R}(p + k)\, G_{-}^{A}(p),$$

$$K_0^{3} = G_{+}^{A}(p + k)\, G_{-}^{A}(p). \quad (5\text{-}19)$$

In a gas, the atoms are nearly free, so that the self energy is much smaller than the kinetic energy. Thus, the G's given by (5-17,18) are nearly singular at $\epsilon = \epsilon_{\underset{\sim}{p}}$. $K_0^{1,2,3}$ must then be small except when ϵ is near $\epsilon_{\underset{\sim}{p}}$. Since K is proportional to K_0, we expect K to peak and diminish the same was as K_0 does.

We are only interested in integrals of the product of $K(\epsilon,\omega)$ and some smooth function of ϵ (see (5-12)). The sum over ϵ'_n in (5-15) will be converted to an integral over real ϵ' and the kernal is expected to be a smooth function of ϵ' because it plays the part of an average scattering amplitude as suggested by the diagrams. The integrals will be dominated by the peaked part of K.

The above consideration leads to the following approximation for the G's.[8] Let

$$G_0^{R,A}(p) \equiv [\epsilon - \epsilon_{\underset{\sim}{p}} \pm i\eta]^{-1} .$$

then

$$G_+^{R,A}(p+k) \approx G_0^{R,A}(p) + \left(\omega - \underset{\sim}{k}\cdot\underset{\sim}{p}\, m^{-1} - E_0 - \Sigma_+^{R,A}(p+k)\right) \frac{\partial}{\partial\epsilon} G_0^{R,A}(p) , \tag{5-20}$$

$$G_-^{R,A}(p) \approx G_0^{R,A}(p) - \Sigma_-^{R,A}(p) \frac{\partial}{\partial\epsilon} G_0^{R,A}(p) . \tag{5-21}$$

Substituting (5-20,21) in (5-19), we have

$$K_0^{\,1} = [G_-^{\,R}(p)^{-1} - G_+^{\,R}(p+k)^{-1}]^{-1} \left(G_+^{\,R}(p+K) - G_-^{\,R}(p)\right)$$

$$\approx \frac{\partial}{\partial\epsilon}\, G_0^{\,R}(p)\,,$$

$$K_0^{\,3} \approx \frac{\partial}{\partial\epsilon}\, G_0^{\,A}(p)\,,$$

$$K_0^{\,2} \approx [-\Sigma_-^{\,A}(p) + \Sigma_+^{\,R}(p+k) - (\omega - \underset{\sim}{k}\cdot\underset{\sim}{p}m^{-1} - E_0)]^{-1}$$

$$\times \Big\{ -2\pi i\, \delta(\epsilon - \epsilon_{\underset{\sim}{p}}) + \frac{\partial}{\partial\epsilon}\, [G_0^{\,R}(p)$$

$$\times \left(\omega - \underset{\sim}{k}\cdot\underset{\sim}{p}m^{-1} - E_0 - \Sigma_+^{\,R}(p+k)\right) - G_0^{\,A}(p)\,\Sigma_-^{\,A}(p)]\Big\}\,. \qquad (5\text{-}22)$$

We now make the further approximation by neglecting the terms involving derivatives since K is to be integrated over a smooth function, whose derivative is small. Thus,

$$K_0^{\,1} \approx K_0^{\,3} \approx 0\,.$$

$$K_0^{\,2} \approx 2\pi i\, \delta(\epsilon - \epsilon_p)/[\omega - E_0 - \underset{\sim}{k}\cdot\underset{\sim}{p}\, m^{-1}$$

$$- \Sigma_+^{\,R}(p+K) + \Sigma_-^{\,A}(p)] \qquad (5\text{-}23)$$

K is proportional to K_0, we have, therefore,

$$K^1 \approx K^3 \approx 0 ,$$

$$K^2(\epsilon, \omega, \underset{\sim}{p}) \approx 2\pi i\, \delta(\epsilon - \epsilon_{\underset{\sim}{p}})\, \phi(\underset{\sim}{p}, \omega) . \qquad (5\text{-}24)$$

We now transform the sum over ϵ'_n in (5-15) to an integral so that we can take advantage of (5-24). Again we replace the sum by an integral enclosing the imaginary axis in ϵ'-plane. (See Fig. 10.) Now we have to know the cuts for $\mathcal{F}_1(\epsilon_n, \epsilon', \omega_n)$ as a function of ϵ', as well as those for $K(\epsilon', \omega_n)$. The singularities of $\mathcal{F}_1(\epsilon, \epsilon', \omega)$ in the space of three complex variables can be located easily by the rule given at the end of Chapter IV. $\mathcal{F}$ has four corners to be hooked to external lines with energies $\epsilon + \omega$, ϵ, $\epsilon' + \omega$, and ϵ', respectively (see Fig. 11). According to the rule, there are seven cuts given by

$$\begin{aligned} &\mathrm{Im}(\epsilon + \omega) = 0, \quad \mathrm{Im}\,\epsilon = 0, \quad \mathrm{Im}(\epsilon' + \omega) = 0, \quad \mathrm{Im}\,\epsilon' = 0, \\ &\mathrm{Im}\,\omega = 0, \quad \mathrm{Im}(\epsilon + \epsilon' + \omega) = 0, \quad \mathrm{Im}(\epsilon - \epsilon') = 0 . \end{aligned} \qquad (5\text{-}25)$$

We are interested in K^2 only, so we restrict our attention to

$$\mathrm{Im}\ \omega > 0, \quad \mathrm{Im}\,\epsilon < 0, \quad \text{and} \quad \mathrm{Im}(\omega + \epsilon) > 0 .$$

On the ϵ'-plane, with definite ϵ_n, ω_n, $\mathcal{F}_1(\epsilon_n, \epsilon', \omega_n)$ has, according to (5-25), cuts along (see Fig. 10)

$$\text{Im } \epsilon' = 0, \quad \text{Im } \epsilon' = -(\epsilon_n + \omega_n), \quad \text{Im } \epsilon' = \epsilon_n, \text{ and } \text{Im } \epsilon' = -\omega_n . \tag{5-26}$$

The region between the cuts $\text{Im } \epsilon' = 0$ and $\text{Im } \epsilon' = -\omega_n$ is the region 2 for $K(\epsilon', \omega)$ (see Fig. 10 and also Figs. 8,9). The function $\mathcal{F}_1(\epsilon_n, \epsilon', \omega_n)$ breaks into three pieces in this region. They are called $\mathcal{F}^1, \mathcal{F}^2$, and $\mathcal{F}^3$, respectively (see Fig. 10), in the three domains bounded by the four cuts. Now we deform the contour C so that the integral is taken above and below the cuts. Therefore

$$\begin{aligned}
&\beta^{-1} \sum_{\epsilon'_n} \mathcal{F}_1(\epsilon_n, \epsilon'_n, \omega_n)\, K(\epsilon'_n, \omega_n)\, e^{\eta\epsilon'_n} \\
&\quad = \int_{-\infty}^{\infty} \frac{d\epsilon'}{2\pi i} \frac{1}{e^{\beta\epsilon'} - 1} \Big[-\mathcal{F}^1(\epsilon_n, \epsilon', \omega_n)\, K^2(\epsilon', \omega_n) \\
&\quad + \mathcal{F}^{12}(\epsilon_n, \epsilon' + \epsilon_n, \omega_n)\, K^2(\epsilon' + \epsilon_n, \omega_n) \\
&\quad + \mathcal{F}^{23}(\epsilon_n, \epsilon' - \epsilon_n - \omega_n, \omega_n)\, K^2(\epsilon' - \epsilon_n - \omega_n, \omega_n) \\
&\quad + \mathcal{F}^3(\epsilon_n, \epsilon' - \omega_n, \omega_n)\, K^2(\epsilon' - \omega_n, \omega_n) \Big]
\end{aligned} \tag{5-27}$$

where $\mathcal{F}^{ij} \equiv \mathcal{F}^i - \mathcal{F}^j$.

Now we let ϵ_n, ω_n approach real values and substitute (5-24) for K^2 in (5-27), then the sum becomes simply

$$F(\underset{\sim}{p}, \underset{\sim}{p}')\, \phi(\underset{\sim}{p}, \omega) , \tag{5-28}$$

where $F(\underset{\sim}{p}, \underset{\sim}{p}')$

$$\equiv \mathcal{F}^{1}(\epsilon, \epsilon_{\underset{\sim}{p}'}, \omega, \underset{\sim}{p}, \underset{\sim}{p}') \left[N(\epsilon_{\underset{\sim}{p}'} + \omega) - N_{p'}\right]$$

$$+ \mathcal{F}^{12}(\epsilon, \epsilon_{\underset{\sim}{p}'}, \omega, \underset{\sim}{p}, \underset{\sim}{p}') \left[N(\epsilon_{\underset{\sim}{p}'} - \epsilon) - N(\epsilon_{\underset{\sim}{p}'} + \omega)\right]$$

$$+ \mathcal{F}^{23}(\epsilon, \epsilon_{\underset{\sim}{p}'}, \omega, \underset{\sim}{p}, \underset{\sim}{p}') \left[N(\epsilon_{\underset{\sim}{p}'} + \epsilon + \omega) - N(\epsilon_{\underset{\sim}{p}'} + \omega)\right] , \qquad (5\text{-}29)$$

and

$$N(\epsilon) \equiv (e^{\beta\epsilon} - 1)^{-1} , \quad N_p \equiv N(\epsilon_{\underset{\sim}{p}}) .$$

The integral equation (5-15) for K^2 continued to real ω and ϵ now becomes, by (5-23,24,28),

$$\phi(\underset{\sim}{p}, \omega) = [\omega - \underset{\sim}{k}\cdot\underset{\sim}{p}\, m^{-1} - E_0 - \Sigma_{+}^{R}(p + k) + \Sigma_{-}^{A}(p)]^{-1}$$

$$\times \left(1 + \int \frac{d^3p'}{(2\pi)^3} F(\underset{\sim}{p}, \underset{\sim}{p}')\, \phi(\underset{\sim}{p}', \omega)\right) . \qquad (5\text{-}30)$$

ϵ is set equal to $\epsilon_{\underset{\sim}{p}}$. Equation (5-12) reduces to

$$\mathcal{S}(\omega + i\eta) = \frac{1}{3}(2j_2 + 1) \int \frac{d^3p}{(2\pi)^3} \left(N(\epsilon_p + \omega) - N_p\right) \phi(\underset{\sim}{p}, \omega) , \qquad (5\text{-}31)$$

and finally the power spectrum $S(\omega)$ is

$$S(\omega) = 2\,\mathrm{Im}\,\mathcal{G}(\omega + i\eta)\,(e^{\beta\omega} - 1)^{-1}$$

$$= \frac{2}{3}\,(2j_2 + 1)\,(e^{\beta\omega} - 1)^{-1}$$

$$\times \int \frac{d^3p}{(2\pi)^3}\,\left(N(\epsilon_p + \omega) - N_p\right)\,\mathrm{Im}\,\phi(\underset{\sim}{p}, \omega) \qquad (5\text{-}32)$$

$$= \frac{1}{3}\,(2j_2 + 1)\int \frac{d^3p}{(2\pi)^3}\,N(\epsilon_p + \omega)\,[-2\,\mathrm{Im}\,\phi(\underset{\sim}{p}, \omega)]\,. \qquad (5\text{-}33)$$

The Eqs. (5-29,30,32,33) formally end the derivation of the expression for the power spectrum. In the next chapter, we shall make further approximations, fix various parameters and describe the procedure and the results of numerical solutions.

VI. FURTHER APPROXIMATION, PHYSICAL INTERPRETATION AND NUMERICAL SOLUTION

In this chapter, we shall consider the simplest diagrams contributing to the kernal $F(\underset{\sim}{p},\underset{\sim}{p}')$ and the self energies Σ_+^R, Σ_-^A, which constitute the input to the integral equation (5-30). We shall discuss the physical meaning of various diagrams. Under further approximations and assumptions, the integral equation becomes simple enough for numerical solution, and the results are discussed.

A. Diffusion of Excitation

We begin by considering the transfer of the internal energy from one atom to another through collisions--collisions via the potential $\tilde{V}^{bc}$, or via the exchange of virtual photons. (See Subsection III.B,4 and Figs. 4d,e.)

The lowest order contribution to $F(\underset{\sim}{p},\underset{\sim}{p}')$ from $\tilde{V}^{bc}$ and the virtual photon is shown in Fig. 12a, and the result of putting such kernal into the integral equation is to generate all the string diagrams like the one shown in Fig. 12b for the Green's function $\mathscr{G}$.

One serious shortcoming of the temperature Green's function method is that the diagrams do not have a straightforward physical interpretation. This is because the time evolution and the statistical averaging are scrambled together and each element in a diagram contains both statistical and dynamical information. For example, a vertex may represent an event as well as a correction to the average of a dozen other events. Nevertheless, one can get some idea of a portion of

the physical information that a diagram contains by breaking up lines, turning parts of the diagram upside down, etc.

One way to break up Fig. 12b is shown in Fig. 12c. It is clear that Fig. 12b does contribute to the average of the sequence of events describing the transfer of the internal energy of atom A to atom C. One can get a diagram contributing to that in Fig. 12b by closing up the ends of each of the external atom lines separately. This procedure represents the averaging over the unperturbed ensemble for each of the atoms in Fig. 12c separately. It is clear that diagrams like Fig. 12b do describe the effect of transfering the internal energy from one atom to another and that the "bubbles" represent independent averages. The name "diffusion of excitation," or "propagation of excitation," or "propagation of a virtual photon" seems to be appropriate to sum up the main effect of the kernal given by Fig. 12a.

One can find the term in $F(\underset{\sim}{p},\underset{\sim}{p}')$ represented by Fig. 12a through our diagram rules and (5-29). The sum of all the string diagrams is

$$\mathcal{G}(\omega + i\eta) = \mathcal{G}'(\omega + i\eta) \left[1 + (D(\underset{\sim}{k},\omega + i\eta) + \tilde{V}_1^{bc}(\underset{\sim}{k})\sqrt{3}\,)\,\mathcal{G}'(\omega + i\eta)\right]^{-1}, \tag{6-1}$$

where $\mathcal{G}'(\omega)$ is the Green's function obtained with Fig. 12a excluded from $F(\underset{\sim}{p},\underset{\sim}{p}')$, or the "undiffused Green's function." $D(k,\omega)$ and $\tilde{V}_J^{bc}$ are defined by (5-4) and (3-10), respectively. Since $\tilde{V}_1^{bc}$ is

an atom-atom scattering amplitude and $\underset{\sim}{k}$, the photon momentum, is much smaller than the momentum of the atoms, then $\tilde{V}_1^{bc}(\underset{\sim}{k}) \approx \tilde{V}_1^{bc}(0)$, the scattering amplitude with internal energy and spin transfer in the forward direction. $D(\underset{\sim}{k}, \omega + i\eta)$, which describes the transient of a damped cavity mode, is approximately constant:

$$D(\underset{\sim}{k}, \omega + i\eta) \approx |g|^2 (2k)^{-1} (i\Gamma_c)^{-1}$$

(see (5-4)). We rewrite (6-1) as

$$\mathscr{D}(\omega + i\eta) = \left[\mathscr{D}'(\omega + i\eta)^{-1} + |g|^2 (2k)^{-1} (i\Gamma_c)^{-1} + \tilde{V}^{bc}(0) \sqrt{3} \right]^{-1}, \tag{6-2}$$

which implies that the effect of the excitation diffusion is the shift and the broadening of the peak of the power spectrum calculated from the undiffused Green's function $\mathscr{D}'(\omega + i\eta)$.

In the frequency range where $\mathscr{D}'(\omega + i\eta)$ is very large and the diffusion of excitation very strong, $\mathscr{D}(\omega + i\eta)$ becomes a constant. The power spectrum $S(\omega)$ (see (5-32)) is then proportional to $(e^{\beta\omega} - 1)^{-1}$, i.e., the source becomes simply a black body emitter in this frequency range. Speaking very roughly, the photons are trapped for a long time and are thermalized by the atoms before they get out. On the other hand, when $\mathscr{D}'$ is small, $\mathscr{D} = \mathscr{D}'$. Thus, the "tail" parts of the spectral lines are affected less by the excitation diffusion because they are off resonance.

We now take a closer look at the question of the photon re-absorption. Let us absorb the constant $\tilde{V}_1^{bc}(0)$ into the definition of $\mathcal{P}'$ and write out the denominator of (6-1) explicitly:

$$\text{denominator} = 1 + \frac{1}{\Gamma_c} \cdot \frac{1}{3}(2j_2 + 1) \frac{|g|^2}{2k}$$

$$\times \int \frac{d^3p}{(2\pi)^3} \left(N_p - N(\epsilon_p + \omega)\right) \left(- \text{Im}\, \phi'(p,\omega)\right)$$

$$+ (i\Gamma_c)^{-1} \text{Re}\, \mathcal{P}' \,, \qquad (6\text{-}3)$$

where we have replaced $\text{Im}\, \mathcal{P}'$ by the integral given by (5-31). $\phi'(\underset{\sim}{p},\omega)$ is the solution of (5-30) with the diagrams in Fig. 12a excluded from $F(\underset{\sim}{p},\underset{\sim}{p}')$.

Except for the last term, which represents a frequency shift, (6-3) is exactly the denominator of (3-12), which is

$$1 + \alpha(\omega)/\Gamma_c \,,$$

where $\alpha(\omega)$ is the absorption rate. The function

$$|g|^2(2k)^{-1} \left[- \text{Im}\, \phi'(\underset{\sim}{p},\omega)\right]$$

which is always positive, is proportional to the absorption or emission rate of a photon by an atom. The integral over N_p, the low level atom occupation number, gives the effect of absorption by lower level

atoms. The integral over $-N(\epsilon_p + \omega)$ gives the "gain" of the virtual photon amplitude when passing by the upper level atoms. There is always a net absorption unless the population is inverted, in which case our temperature Green's function method is not defined.

Having gone through the reabsorption process in some detail, we like to emphasize again that it should be viewed as one of the important processes contributing to the diffusion of excitation. It is the diffusion of excitation, not the photon, that is important.

B. Additional Implications of the Cavity Mode Propagator

The cavity mode propagator D used in the last section is a temperature Green's function, and it implies more than just the transfer of internal energy. In addition, it automatically implies the existence of cavity modes in thermal equilibrium with the atoms. This seems to be inconsistent with our assumption that the wall of the cavity is transparent. However, the important question is not whether the cavity modes are or are not thermally excited. After all, we have a large thermal reservoir to distribute the atom population and any additional system in thermal equilibrium with the atoms simply implies a larger reservoir, which has no effect except introducing new perturbation to the atom currents. Thus, the important question is whether the additional perturbation is small compared to the other perturbations already included in the model. The answer will be clear after we examine the diagrams discussed in the last section further and analyze the self energy diagram Fig. 13, in which the propagator D also plays a part.

Let us analyze Fig. 13 first. If one calculates Fig. 13, one would end up calculating two effects; first, the temperature independent "true" self energy, and second, the forward scattering amplitude averaged over the thermal equilibrium cavity model population (see Fig. 14a,b, which are not temperature Green's function diagrams but ordinary diagrams showing the events). The second effect is the additional fluctuation, which gives rise to the well known dissipation due to the stimulated emission.

In fact, every factor D may be thought of as having two effects; first, the propagation of a virtual photon in the ordinary sense, and second, an average over the external lines created by breaking the wavy line.

If we break a wavy line in a string diagram like the one shown in Fig. 12b, we get two disconnected pieces, which contribute to the square of the amplitude of a process in which a cavity mode excites an atom and the internal energy thus created then diffuses away to other atoms. Figure 12d shows such a process.

Now the implications of D apart from describing the exchange of the internal energy are clear. First, the cavity modes cause additional fluctuation and the stimulated emission results. This additional fluctuation is usually much less than that due to collisions. Second, the cavity modes act as a source, and therefore must also act as a sink of the atom internal energy. This implies a bigger reservoir and has no effect on the result of the previous section.

In the rest of this chapter we shall limit our discussion to the effect of collisions on the structure of the kernal $F(\underset{\sim}{p},\underset{\sim}{p}')$ and the self energies Σ_+^R, and Σ_-^A.

C. The Self Energies

In this section we shall evaluate the self energies Σ_+^R and Σ_-^A in second order of the interaction potentials given by (3-8,9,10). The first order terms will be ignored for the following reasons. The first order terms are the Hartree and the Hartree-Fock corrections, which are small for a dilute gas. More important, the interaction potentials are in general unknown or undefined. The second order terms may be identified as proportional to various cross sections, for which more definite statements can be made.

Figure 15 shows the second order diagrams representing the following terms. For $\Sigma_+^R(p + k)$, Figs. 15a,b,c give

$$\text{a.} \quad \int \frac{d^3p'}{(2\pi)^3} \frac{d^3p''}{(2\pi)^3} (2j_1 + 1) N_{p''} |V^{bc}(\underset{\sim}{p} - \underset{\sim}{p}')|^2 \times \delta_+(\epsilon_{\underset{\sim}{p}} + \epsilon_{\underset{\sim}{p}''} - \epsilon_{\underset{\sim}{p}+\underset{\sim}{p}''-\underset{\sim}{p}'} - \epsilon_{\underset{\sim}{p}'}) \quad ,$$

$$\text{b.} \quad \int \frac{d^3p'}{(2\pi)^3} \frac{d^3p''}{(2\pi)^3} (2j_2 + 1) N^+_{p''} |V^{cc}(\underset{\sim}{p} - \underset{\sim}{p}')|^2 \times \delta_+(\epsilon_{\underset{\sim}{p}} + \epsilon_{\underset{\sim}{p}''} - \epsilon_{\underset{\sim}{p}+\underset{\sim}{p}''-\underset{\sim}{p}'} - \epsilon_{\underset{\sim}{p}'}) \quad ,$$

$$\text{c.} \quad \int \frac{d^3p'}{(2\pi)^3} \frac{d^3p''}{(2\pi)^3} (2j_1 + 1) N_{p''} |\tilde{V}^{bc}(\underset{\sim}{p} - \underset{\sim}{p}')|^2 \times \delta_+(\epsilon_{\underset{\sim}{p}} + \epsilon_{\underset{\sim}{p}''} - \epsilon_{\underset{\sim}{p}+\underset{\sim}{p}''-\underset{\sim}{p}'} - \epsilon_{\underset{\sim}{p}'}) \quad . \qquad (6\text{-}5)$$

For $\Sigma_-^A(p)$, we have, from Figs. 15d,e,f,

$$\text{d.} \quad \int \frac{d^3p'}{(2\pi)^3} \frac{d^3p''}{(2\pi)^3} (2j_1 + 1) N_{p''} |V^{bb}(\underset{\sim}{p} - \underset{\sim}{p}')|^2$$

$$\times \delta_-(\epsilon_{\underset{\sim}{p}} + \epsilon_{\underset{\sim}{p}''} - \epsilon_{\underset{\sim}{p}+\underset{\sim}{p}''-\underset{\sim}{p}'} - \epsilon_{\underset{\sim}{p}'}) \quad ,$$

$$\text{e.} \quad \int \frac{d^3p'}{(2\pi)^3} \frac{d^3p''}{(2\pi)^3} (2j_2 + 1) N^+_{p''} |V^{bc}(\underset{\sim}{p} - \underset{\sim}{p}')|^2$$

$$\times \delta_-(\epsilon_{\underset{\sim}{p}} + \epsilon_{\underset{\sim}{p}''} - \epsilon_{\underset{\sim}{p}+\underset{\sim}{p}''-\underset{\sim}{p}'} - \epsilon_{\underset{\sim}{p}'}) \quad ,$$

$$\text{f.} \quad \int \frac{d^3p'}{(2\pi)^3} \frac{d^3p''}{(2\pi)^3} (2j_2 + 1)^2/(2j_1 + 1) N^+_{p''} |\tilde{V}^{bc}(\underset{\sim}{p} - \underset{\sim}{p}')|^2$$

$$\times \delta_-(\epsilon_{\underset{\sim}{p}} + \epsilon_{\underset{\sim}{p}''} - \epsilon_{\underset{\sim}{p}+\underset{\sim}{p}''-\underset{\sim}{p}'} - \epsilon_{\underset{\sim}{p}'}) \quad ; \qquad (6\text{-}6)$$

we have used the abbreviations

$$N^+_p \equiv \left(e^{\beta(\epsilon_p+E_0)} - 1\right)^{-1} = \text{the occupation number per state in}$$

the upper level $\approx e^{-\beta(\epsilon_p+E_0)}$,

$$\delta_\pm(x) \equiv 1/(x \pm i\eta) \, ,$$

and also

$$|V|^2 = \sum_J |V_J|^2 \, . \qquad (6\text{-}7)$$

The V_J's are the potentials for definite spin transfer defined by (3-9,10). In calculating (6-5,6), only the first power of the occupation numbers are kept. Exchange diagrams such as Fig. 16 are ignored. For future reference, we define $\tilde{\Sigma}(p)$ and $\Sigma(p)$ by

$$\Sigma_+^R(p + k) - \Sigma_-^A(p) \equiv \Sigma(p) + \tilde{\Sigma}(p) , \qquad (6\text{-}8)$$

where $\tilde{\Sigma}(p)$ is the contribution from $\tilde{\tilde{V}}^{bc}$, the potential for the scattering involving internal energy transfer.

D. The Kernal $F(\underset{\sim}{p},\underset{\sim}{p}')$

The kernal $F(\underset{\sim}{p},\underset{\sim}{p}')$ can be found from (5-29) after $\mathcal{H}^1$, $\mathcal{H}^2$, and $\mathcal{H}^3$ are calculated from the diagrams. There are two first order diagrams (see Fig. 17). Figure 17a plays a part in the "diffusion of excitation" process discussed in Section A of this chapter and its effect is given in (6-2), which can be carried out at the end of all calculations. Figure 19 shows the second order diagrams which we shall calculate. Figure 18 may look like a second order contribution to $F(\underset{\sim}{p},\underset{\sim}{p}')$ from $\tilde{\tilde{V}}^{bc}$, but it must not be included because it simply generates a part of the "string diagrams" (see Fig. 12) generated by the first order kernal shown in Fig. 17a or 12a.

Straightforward algebra leads to the following expression for $F(\underset{\sim}{p},\underset{\sim}{p}')$ due to the diagrams shown in Figs. 17b and 19 :

$$F(\underset{\sim}{p},\underset{\sim}{p}') = [V^{bc}(p - p')]\ (N^{\dagger}_{p'} - N_{p'})$$

$$+ \ i\int \frac{d^3p''}{(2\pi)^3}\ [V^{bc}(\underset{\sim}{p} - \underset{\sim}{p}')\ V^{bb}(\underset{\sim}{p}' - \underset{\sim}{p})]\ (2j_1 + 1)\ N_{p''}$$

$$\times\ 2\pi\ \delta(\epsilon_{\underset{\sim}{p}} + \epsilon_{\underset{\sim}{p}''} - \epsilon_{\underset{\sim}{p}+\underset{\sim}{p}''-\underset{\sim}{p}'} - \epsilon_{\underset{\sim}{p}'})$$

$$+ \ i\int \frac{d^3p''}{(2\pi)^3}\ [V^{cc}(\underset{\sim}{p} - \underset{\sim}{p}')\ V^{bc}(\underset{\sim}{p}' - \underset{\sim}{p})]\ (2j_2 + 1)\ N^{\dagger}_{p''}$$

$$\times\ 2\pi\ \delta(\epsilon_{\underset{\sim}{p}} + \epsilon_{\underset{\sim}{p}''} - \epsilon_{\underset{\sim}{p}+\underset{\sim}{p}''-\underset{\sim}{p}'} - \epsilon_{\underset{\sim}{p}'})\ . \qquad (6\text{-}9)$$

We have used the shorthand [V], and [VV'] in (6-9) to denote

$$[V^{bc}] = \sum_{J'} V_{J'}{}^{bc}\ R_{J'}\ ,$$

and

$$[VV'] = \sum_{J'} V_{J'}\ V'_{J'}\ R_{J'}\ , \qquad (6\text{-}10)$$

respectively, where

$$R_{J'} \equiv [(2j_1 + 1)\ (2j_2 + 1)]^{\frac{1}{2}}\ (-)^{1+J'-j_1-j_2}$$

$$\times \begin{Bmatrix} j_1 & j_2 & 1 \\ j_2 & j_1 & J' \end{Bmatrix}\ . \qquad (6\text{-}11)$$

The appearance of a 6j symbol is due to the summation over four Wigner coefficients as required by (5-14). Notice that $\tilde{V}^{bc}$ does not

appear in $F(\underset{\sim}{p},\underset{\sim}{p}')$. The equations (6-8,9) constitute the input to the integral equation for $\phi(\underset{\sim}{p},\omega)$.

What is the physical meaning of $\phi(\underset{\sim}{p},\omega)$? Recall that ϕ is related to the vertex function K through (5-24):

$$K^2 = 2\pi i\, \delta(\epsilon - \epsilon_p)\, \phi(\underset{\sim}{p},\omega) . \qquad (6\text{-}11)$$

The diagram for the vertex function is in Fig. 7. It has three ends, two for the incoming and out-going atom and the third for the current operator to be coupled to a photon in the vacuum. Roughly speaking, the vertex function is proportional to the average of the product

(the amplitude of finding the atom in the upper level)
× (that of finding it in the lower level)*. (6-12)

The factor $\delta(\epsilon - \epsilon_p)$ puts the atom on its "energy shell," i.e., the atom is almost free. $\phi(\underset{\sim}{p},\omega)$ therefore sums up what is happening to the atom when a photon is emitted or absorbed. The self energies and the kernal together describe the correction to the vertex function due to collisions. As an example, Fig. 20 shows that an atom is colliding with another atom while emitting a photon. The events shown in a and c are included in the self energy terms while that in b is generated by the kernal.

The self energies always give a dissipative effect and the kernal must have the effect of compensating such dissipation to some extent.

This can be seen by the following argument. If the internal state of the atom is not disturbed by the collisions, then the product (6-12) must not be dissipated at all. Therefore, the presence of a dissipating term implies that of a compensatory term.

E. Limit of No Spin Transfer, Collision Narrowing

To extract still more explicit information out of the integral equation (5-30) and then solve it, we have to restrict our discussion to very special cases where the expressions for the self energies and the kernal are further simplified.

Unlike those appearing in (6-5,6,7) for the self energies, the potentials appearing in the expression (6-9) for the kernal do not appear in the form $|V|^2$. They only appear as the products of different V's and therefore cannot be related to some cross sections. To proceed, let us make the following restriction.

First, we drop the first order term in (6-9). Then let the $J' = 0$ term be separated from the sum (6-10) and, utilizing the identity

$$\begin{Bmatrix} j_1 & j_2 & J \\ j_2 & j_1 & 0 \end{Bmatrix} = (-)^{j_1 + j_2 + J} \times [(2j_1 + 1)(2j_2 + 1)]^{-\frac{1}{2}} , \qquad (6\text{-}12)$$

we have, from (6-10),

$$[VV'] = V_0 V'_0 + \sum_{J' \neq 0} J_{J'} V'_{J'} R_{J'} . \qquad (6\text{-}13)$$

The V_0's are the amplitudes for collisions with no spin transfer, i.e., collisions in which the internal states of the colliding atoms are not affected. If we restrict our discussion to the limiting cases where such collisions dominate and also are independent of the level of the atoms, i.e.,

$$V_0^{bb} \approx V_0^{bc} \approx V_0^{cc} \equiv V_0 , \tag{6-14}$$

we have

$$[VV'] \approx |V_0|^2 . \tag{6-15}$$

These restrictions effectively eliminate the complications, and hence much of the essential features, of having two species of atoms and of having arbitrary spins. Under the assumptions (6-14,15), we obtain from (6-6,7,8,9)

$$F(\underset{\sim}{p},\underset{\sim}{p}') = i\int \frac{d^3p''}{(2\pi)^3} |V_0(\underset{\sim}{p} - \underset{\sim}{p}')|^2 \left\{ N_{p''}(2j_1 + 1) + N^{+}_{p''}(2j_2 + 1) \right\}$$

$$\times 2\pi\, \delta(\epsilon_{\underset{\sim}{p}} + \epsilon_{\underset{\sim}{p}''} - \epsilon_{\underset{\sim}{p}+\underset{\sim}{p}''-\underset{\sim}{p}'} - \epsilon_{\underset{\sim}{p}'}) , \tag{6-16}$$

$$\mathrm{Re}\ \Sigma(p) = 0 , \tag{6-17}$$

$$i\ \mathrm{Im}\ \Sigma(p) = -\int \frac{d^3p'}{(2\pi)^3} F(\underset{\sim}{p},\underset{\sim}{p}') . \tag{6-18}$$

The integral equation (5-30) may now be written as

$$\left(\omega - \underset{\sim}{k}\cdot\underset{\sim}{p}\, m^{-1} - E_0 - \tilde{\Sigma}(p)\right) \phi(\underset{\sim}{p},\omega) = 1 + \int \frac{d^3p'}{(2\pi)^3}$$

$$\times F(\underset{\sim}{p},\underset{\sim}{p}') \left(\phi(\underset{\sim}{p}',\omega) - \phi(\underset{\sim}{p},\omega)\right) . \qquad (6\text{-}19)$$

We make no attempt to simplify $\tilde{\Sigma}(p)$, (see (6-8)) the self energy terms due to the scattering with internal energy transfer.

If we define a function $f(\underset{\sim}{p},\omega)$ by

$$f(\underset{\sim}{p},\omega) \equiv i\, N_p \phi(\underset{\sim}{p},\omega) = i\, e^{-\beta\epsilon_p} \phi(\underset{\sim}{p},\omega) , \qquad (6\text{-}20)$$

then (6-19) takes the form

$$- i \left[\omega - \underset{\sim}{k}\cdot\underset{\sim}{p}\, m^{-1} - E_0 - \tilde{\Sigma}(p)\right] f(\underset{\sim}{p},\omega) = N_p$$

$$+ \int \frac{d^3p'}{(2\pi)^3} \left[- i\, F(\underset{\sim}{p},\underset{\sim}{p}')\, f(\underset{\sim}{p}',\omega) + i\, F(\underset{\sim}{p}',\underset{\sim}{p})\, f(\underset{\sim}{p},\omega)\right] . \qquad (6\text{-}21)$$

Equation (6-21) has the form of a master equation. $f(\underset{\sim}{p},\omega)$ is the Boltzmann function and $-iF(\underset{\sim}{p},\underset{\sim}{p}')$ is the transition probability per unit time from the state $\underset{\sim}{p}'$ to the state $\underset{\sim}{p}$. $\tilde{\Sigma}(p)$ gives an additional dissipation and frequency shift. The physical picture now simplifies to that of a gas of atoms, each carrying an oscillating dipole, colliding and emitting photons independently. The function $-2\,\mathrm{Im}\,\phi(\underset{\sim}{p},\omega)$ is the power spectrum generated by an atom with momentum

$\underset{\sim}{p}$. The total power spectrum is obtained by integrating over $\underset{\sim}{p}$ weighted by the population distribution function (see (5-33)).

Before solving the integral equation (6-19), let us anticipate the solution for extreme cases.

First, if $F(\underset{\sim}{p},\underset{\sim}{p}')$ is very small (compared to $\underset{\sim}{k}\cdot\underset{\sim}{p}/m$), then

$$\phi(\underset{\sim}{p},\omega) \approx [\omega - E_0 - \underset{\sim}{k}\cdot\underset{\sim}{p}\, m^{-1} - \tilde{\Sigma}(p)]^{-1} \quad . \tag{6-22}$$

For small $\Sigma(p)$ one would have a Doppler line shape. For large $\tilde{\Sigma}(p)$, i.e., when the collisions involving internal energy transfer dominate, the power spectrum has the shape of the imaginary part of the Plasma Dispersion Function,[9] if $\tilde{\Sigma}(p)$ is a slowly varying function of p . It approaches a Lorentzian when $\tilde{\Sigma}(p)$ becomes much larger than the Doppler width. Therefore, the integral equation is uninteresting when $F(\underset{\sim}{p},\underset{\sim}{p}')$ is small.

Second, if $F(\underset{\sim}{p},\underset{\sim}{p}')$ is very large and $\tilde{\Sigma}(p)$ is very small, then each atom is bound by its neighbors but its internal state is not affected by collisions. We then expect some sort of "Mössbauer Effect" so that the power spectrum becomes much narrower than the Doppler shape. This is the "collision narrowing" phenomenon.[10]

Third, when both $F(\underset{\sim}{p},\underset{\sim}{p}')$ and $\tilde{\Sigma}(p)$ are large, we have both the narrowing and broadening effects. As we shall see, the broadening due to $\tilde{\Sigma}(p)$ tends to be dominating.

F. Numerical Solution

We shall first solve the integral equation (6-19) and calculate the power spectrum for zero $\tilde{\Sigma}(p)$ so that the collision narrowing can be observed as we increase the transition rate $F(\underset{\sim}{p},\underset{\sim}{p}')$. Then we increase $\tilde{\Sigma}(p)$ to see the broadening and the shift.

To write everything in terms of dimensionless quantities, we define the following symbols:

$$\underset{\sim}{y} = \underset{\sim}{p}/(\text{Thermal momentum}) , \tag{6-23}$$

where

$$\text{Thermal momentum} = (2m/\beta)^{\frac{1}{2}} \equiv (2mkT)^{\frac{1}{2}} ;$$

$$\lambda = (\omega - E_0)/(\text{Doppler width}),$$

$$\Sigma'(y) = \Sigma(p)/(\text{Doppler width}),$$

$$\tilde{\Sigma}'(y) = \Sigma(p)/(\text{Doppler width}), \tag{6-24}$$

where

$$\text{Doppler width} = (E_0/m) \cdot (\text{Thermal momentum});$$

$$\phi'(\underset{\sim}{y},\lambda) = (\text{Doppler width}).\ \phi(\underset{\sim}{p},\omega) , \tag{6-25}$$

$$F'(\underset{\sim}{y},\underset{\sim}{y}') = (2\pi)^{-3}\ (\text{Thermal momentum})^3\ (\text{Doppler width})^{-1}\ F(\underset{\sim}{p},\underset{\sim}{p}') \tag{6-26}$$

The integral equation (6-19) then takes the form:

$$\phi'(\underset{\sim}{y},\lambda) = [\lambda - \underset{\sim}{y}\cdot\hat{k} - \tilde{\Sigma}'(y) - \Sigma'(y)]^{-1}$$

$$\times [1 + \int d^3y'\ F'(\underset{\sim}{y},\underset{\sim}{y'})\ \phi'(\underset{\sim}{y'},\lambda)] \ . \qquad (6\text{-}27)$$

The explicit form of the kernal $F'(\underset{\sim}{y},\underset{\sim}{y'})$ can be worked out from (6-16):

$$F'(\underset{\sim}{y},\underset{\sim}{y'}) = i\,\xi\,q^{-1}\ \exp - (\hat{q}\cdot\underset{\sim}{y'})^2 \ , \qquad (6\text{-}28)$$

$$\xi = n\,E_0^{-1}\,\pi^{-\frac{1}{2}}\,\sigma(q) \ , \qquad (6\text{-}29)$$

where

$$\underset{\sim}{q} \equiv \underset{\sim}{y'} - \underset{\sim}{y}$$

is the momentum transfer in units of thermal momentum, n = the total number of atoms per volume, and $\sigma(q)$ is the c.m. differential cross section (in the Born approximation) for the scattering not affecting the internal state of the atoms. ξ is approximately the number of atoms in a cylinder of cross area σ and one wavelength long.

The self energy terms $\Sigma'(y)$ and $\tilde{\Sigma}'(y)$ are given by

$$\Sigma'(y) = \int d^3y'\ F'(\underset{\sim}{y},\underset{\sim}{y'}) \ ,$$

$$\Sigma'(y) = \int d^3y'\ \tilde{F}'(\underset{\sim}{y},\underset{\sim}{y'}) \ , \qquad (6\text{-}30)$$

where $\tilde{F}'(\underset{\sim}{y},\underset{\sim}{y'})$ is given by

$$\text{Re } \tilde{F}' = \tilde{\xi}^{-}(2\pi q)^{-1} \int \frac{du}{u} \exp - (u - \hat{q}\cdot\underset{\sim}{y}')^2 ,$$

$$\text{Im } \tilde{F}' = -\tfrac{1}{2} \tilde{\xi}^{+} q^{-1} \exp - (\hat{q}\cdot\underset{\sim}{y}')^2 , \qquad (6\text{-}31)$$

and

$$\tilde{\xi}^{\pm} = \pi^{-\frac{1}{2}} E_0^{-1} [n_b \pm n_c (2j_2 + 1)/(2j_1 + 1)] \tilde{\sigma}(q) . \qquad (6\text{-}32)$$

$\tilde{\sigma}(q)$ is the c.m. differential cross section for the scattering with internal energy transfer. $n_b(n_c)$ is the number of atoms in the lower (upper) level per volume.

The integral equation (6-27) can then be solved and the function

$$S'(\lambda) = \int d^3y \; e^{-y^2} \; \phi'(\underset{\sim}{y},\lambda) \qquad (6\text{-}33)$$

calculated with the input parameters $\lambda, \xi, \tilde{\xi}^{\pm}$. $S'(\lambda)$ is proportional to the power spectrum $S(\omega)$. The proportionality factor is uninteresting. The correction (6-1) will not be carried out since its consequence is obvious.

The integral equation is solved by first reducing it to a set of simulteneous linear equations through expanding $\phi'(y,\lambda)$ in terms of Legendre and Laguerre polynomials, and then solving the resulting set of linear equations. The detail is described in Appendix B. Before presenting the results, it seems proper to repeat here the meaning of the parameters.

λ is the frequency in units of Doppler width measured from E_0, the unperturbed atomic transition frequency. ξ is approximately the total number of atoms in a cylinder of length E_0^{-1} and cross area $\sigma(q)$. $\tilde{\xi}^+$ is the same as ξ except that the cylinder has a cross sectional area $\tilde{\sigma}(q)$. $\tilde{\xi}^-$ is roughly the number difference of the upper and lower level atoms in the cylinder. The order of magnitude of the size of the cylinder is about 10^{-20} c.c., if we take $E_0 \sim 2$ ev. and a cross sectional area 10^{-15} cm^2.

For large q the parameters ξ and $\tilde{\xi}^+_-$ are cut off arbitrarily by the factor $(1 + 4q^2)^{-2}$. This corresponds to assuming that the cross sections have the momentum transfer dependence $(1 + 4q^2)^{-2}$. See (6-29) and (6-32).

The computed $S'(\lambda)$ is plotted vs. λ in Figs. 21, and 22. For the curves in Fig. 21, $\tilde{\xi}^+_- = 0$, corresponding to no collisions involving internal energy transfer. We see that the lines become sharper for increasing ξ. Figure 22 shows the effect of a non-zero $\tilde{\xi}^+_-$, corresponding to a finite cross section for collisions involving internal energy transfer.

Let us summarize what has been done in the previous chapter and this chapter.

We have discussed the power spectrum $S(\omega)$, which is related to the photon amplitude correlation function through (3-1). We first expressed S in terms of the discontinuity of the Green's function $\mathscr{G}(\omega)$ in (5-3). Then $\mathscr{G}(\omega)$ was related to the vertex function which satisfies an integral equation represented by Fig. 7. We arrived at

the general form of this integral equation for a dilute gas (5-30) at the end of the last chapter. In this chapter, we made many simplifying assumptions to make the physical implication of the integral equation explicit. We then solved the equation under special conditions.

Our discussion on the amplitude correlation function is completed. We now turn our attention to the intensity correlation function.

VII. TEMPERATURE GREEN'S FUNCTIONS WITH THREE TIME ARGUMENTS

The purpose of this chapter is two-fold. First, in order to calculate the intensity correlation function in the next chapter by the temperature Green's function method, we need a few general equations. This chapter will supply these equations. Second, the discussion in Section IV.C on the analytic structure of an arbitrary temperature Green's function is only a brief sketch. In this chapter, a more detailed analysis of the three end temperature Green's function will provide a better understanding of the general techniques.

Our analysis will be based entirely on the expansion of the temperature Green's function in terms of the matrix elements between the energy eigenstates of the system.

A. Fourier Series

The general form of a temperature Green's function with three ends is

$$K = Z^{-1} \operatorname{Tr} \left\{ e^{-\beta H} T(\hat{A}(\tau_1) \hat{B}(\tau_2) \hat{C}(\tau_3)) \right\} , \tag{7-1}$$

where $\hat{A}(\tau_1) \equiv e^{\tau_1 H} A e^{-\tau_1 H}$ etc., and

$$\beta \geq \tau_1, \tau_2, \tau_3 \geq 0 . \tag{7-2}$$

Without losing much generality, we shall assume that none of the operators A, B, C is a fermion operator.

The ensemble is stationary, so that K is a function of two variables,

$$t_1 \equiv \tau_1 - \tau_2 \ ,$$

and

$$t_2 \equiv \tau_2 - \tau_3 \ . \tag{7-3}$$

There are $3! = 6$ different orderings of the imaginary times τ_1, τ_2, τ_3. Let us divide them into two cycles. Cycle 1 consists of the orderings (1,2,3), (2,3,1), and (3,1,2). Cycle 2 consists of the orderings (3,2,1), (2,1,3), and (1,3,2). In terms of the matrix elements of A, B, C between eignestates of H, the cycle 1 orderings give

$$\begin{aligned} K(\text{Cycle 1}) = Z^{-1} \sum_{a,b,c} A_{ab} B_{bc} C_{ca} \Big[& e^{-\beta E_a} \theta(1\,2\,3) \\ & + e^{-\beta E_b} \theta(2\,3\,1) + e^{-\beta E_b} \theta(3\,1\,2) \Big] \\ & \times e^{E_{ab}\tau_1 + E_{bc}\tau_2 + E_{ca}\tau_3} \ , \end{aligned} \tag{7-4}$$

where

$$\theta(1\,2\,3) = \theta(\tau_1 - \tau_2)\,\theta(\tau_2 - \tau_3), \text{ etc.,}$$

and (7-5)

$$E_{ab} = E_a - E_b \ .$$

The three terms in (7-4) are separately defined in the regions I, II, and III shown in Fig. 23. The boundaries of the regions are defined by the step functions and the restrictions (7-2):

$$\text{Region I :} \quad \theta(1\,2\,3) \to \theta(t_1)\,\theta(t_2)\,\theta(\beta - t_1 - t_2)\,,$$

$$\text{Region II :} \quad \theta(2\,3\,1) \to \theta(t_1 + \beta)\,\theta(t_2)\,\theta(-t_1 - t_2)\,, \qquad (7\text{-}6)$$

$$\text{Region III :} \quad \theta(3\,1\,2) \to \theta(t_1)\,\theta(\beta + t_2)\,\theta(-t_1 - t_2)\,.$$

The values of K(cycle 1) in II and III are related to those in I by

$$K(t_1,t_2) = K(t_1 - \beta, t_2)$$

$$= K(t_1, t_2 - \beta) \qquad (7\text{-}7)$$

for $(t_1,t_2) \in I$. Equation (7-7) is obtained from (7-4,6) by straightforward substitution. Therefore, $K(t_1,t_2)$ may be written as a Fourier series :

$$K(t_1,t_2) = \beta^{-2} \sum_{\omega_1,\omega_3} e^{-\omega_1 t_1 + \omega_3 t_2}\, K(\text{cycle 1} ; \omega_1,\omega_2), \qquad (7\text{-}8)$$

where

$$\omega_1,\ \omega_3 = (2\pi i/\beta) \times \text{integer}. \qquad (7\text{-}9)$$

and

$$K(\text{cycle 1} ; \omega_1,\omega_2) = \int_0^{\beta} dt_2 \int_0^{\beta - t_2} dt_1\, e^{\omega_1 t_1 - \omega_3 t_2}\, K(t_1,t_2)\,. \qquad (7\text{-}10)$$

Substituting (7-4) into (7-10), we obtain

$$K(\text{cycle } 1 ; \omega_1, \omega_2, \omega_3)$$

$$= - Z^{-1} \sum_{a,b,c} A_{ab} B_{bc} C_{ca} \left[\frac{e^{-\beta E_a}}{(\omega_1 + E_{ab})(\omega_3 + E_{ca})} + \frac{e^{-\beta E_b}}{(\omega_1 + E_{ab})(\omega_2 + E_{bc})} + \frac{e^{-\beta E_c}}{(\omega_2 + E_{bc})(\omega_3 + E_{ca})} \right] . \qquad (7\text{-}11)$$

We have introduced a new variable

$$\omega_2 \equiv - \omega_1 - \omega_3 \qquad (7\text{-}12)$$

to make the expression (7-11) appear more symmetrical.

We go through the above steps in the same fashion for the Cycle 2 orderings. We obtain, similar to (7-4),

$$K(\text{cycle } 2) = Z^{-1} \sum_{a,b,c} C_{ac} B_{cb} A_{ba} \left[e^{-\beta E_a} \theta(3\ 2\ 1) + e^{-\beta E_c} \theta(2\ 1\ 3) + e^{-\beta E_b} \theta(1\ 3\ 2) \right] e^{E_{ac} \tau_3 + E_{cb} \tau_2 + E_{ba} \tau_1} . \qquad (7\text{-}13)$$

The three terms in (7-13) are separately defined in Regions I, II, and III shown in Fig. 24. The boundaries are defined by the step functions in (7-13) and the restrictions (7-2) :

$$\begin{aligned} &\text{Region I :} && \theta(3\ 2\ 1) \to \theta(t_1 + t_2 + \beta)\, \theta(- t_1)\, \theta(- t_2) , \\ &\text{Region II :} && \theta(2\ 1\ 3) \to \theta(\beta - t_2)\, \theta(t_1 + t_2)\, \theta(- t_1) , \\ &\text{Region III:} && \theta(1\ 3\ 2) \to \theta(- t_2)\, \theta(t_1 + t_2)\, \theta(\beta - t_1) . \end{aligned} \qquad (7\text{-}14)$$

The values of K(Cycle 2) in I, II, and III are related by

$$K(t_1,t_2) = K(t_1 + \beta, t_2)$$

$$= K(t_1, t_2 + \beta) , \qquad (7\text{-}15)$$

for $(t_1,t_2) \in I$. Thus, $K(t_1,t_2)$ may be written as a Fourier series. Similar to (7-11) we obtain $K(\text{Cycle } 2 ; \omega_1, \omega_2, \omega_3)$. The sum of K(Cycle 1) and K(Cycle 2) gives

$$K(\omega_1,\omega_2,\omega_3) = - Z^{-1} \sum_{a,b,c} \left\{ A_{ab} B_{bc} C_{ca} \left[\frac{e^{-\beta E_a}}{(\omega_1 + E_{ab})(\omega_3 + E_{ca})} + \frac{e^{-\beta E_b}}{(\omega_1 + E_{ab})(\omega_2 + E_{bc})} + \frac{e^{-\beta E_c}}{(\omega_2 + E_{bc})(\omega_3 + E_{ca})} \right] \right.$$

$$\left. + C_{ac} B_{cb} A_{ba} \left[\frac{e^{-\beta E_a}}{(\omega_1 + E_{ba})(\omega_3 + E_{ac})} + \frac{e^{-\beta E_b}}{(\omega_1 + E_{ba})(\omega_2 + E_{cb})} + \frac{e^{-\beta E_c}}{(\omega_2 + E_{cb})(\omega_3 + E_{ac})} \right] \right\} . \qquad (7\text{-}16)$$

The analytic continuation of K into the space of two complex variables is then obtained by letting $\omega_{1,2,3}$ be complex and keep $\omega_1 + \omega_2 + \omega_3 = 0$.

B. Spectral Functions and the Spectral Representation

The expansion (7-16) is the spectral representation we look for. To write it in a better form, let us define, for real $\omega_1, \omega_2, \omega_3$, the spectral functions ρ_{12}, ρ_{23}, and ρ_{31} as,

$$\rho_{12}(\omega_1,\omega_2) = (2\pi)^2 \sum_{a,b,c} e^{-\beta E_b} [A_{ab}B_{bc}C_{ca}\,\delta(\omega_1+E_{ab})\,\delta(\omega_2+E_{bc}) + A_{ba}\,B_{cb}\,C_{ac}\,\delta(\omega_1+E_{ba})\,\delta(\omega_2+E_{cb})]\,Z^{-1},$$

$$\rho_{23}(\omega_2,\omega_3) = (2\pi)^2 \sum_{a,b,c} e^{-\beta E_c} [A_{ab}B_{bc}C_{ca}\,\delta(\omega_2+E_{bc})\,\delta(\omega_3+E_{ca}) + A_{ba}\,B_{cb}\,C_{ac}\,\delta(\omega_2+E_{cb})\,\delta(\omega_3+E_{ac})]\,Z^{-1},$$

$$\rho_{31}(\omega_3,\omega_1) = (2\pi)^2 \sum_{a,b,c} E^{-\beta E_a} [A_{ab}B_{bc}C_{ca}\,\delta(\omega_1+E_{ab})\,\delta(\omega_3+E_{ca}) + A_{ba}\,B_{cb}\,C_{ac}\,\delta(\omega_1+E_{ba})\,\delta(\omega_3+E_{ac})]\,Z^{-1}, \qquad (7\text{-}17)$$

where

$$\omega_1 + \omega_2 + \omega_3 = 0 .$$

Then K has the spectral representation:

$$K(\omega_1,\omega_2,\omega_3) = -\int \frac{d\omega'_1}{2\pi}\,\frac{d\omega'_2}{2\pi}\,\frac{\rho_{12}(\omega'_1,\omega'_2)}{(\omega_1-\omega'_1)(\omega_2-\omega'_2)} - \int \frac{d\omega'_2}{2\pi}\,\frac{d\omega'_3}{2\pi}\,\frac{\rho_{23}(\omega'_2,\omega'_3)}{(\omega_2-\omega'_2)(\omega_3-\omega'_3)} - \int \frac{d\omega'_3}{2\pi}\,\frac{d\omega'_1}{2\pi}\,\frac{\rho_{31}(\omega'_3,\omega'_1)}{(\omega_3-\omega'_3)(\omega_1-\omega'_1)} \quad . \tag{7-18}$$

We may represent K by a diagram (see Fig. 25). The three energy variables are associated with the three ends A, B, and C. The ρ's are not independent. In fact, if we define ρ^{I}, and ρ^{II} by

$$\rho^{I} = Z^{-1}(2\pi)^2 \sum_{a,b,c} e^{-\beta E_a} A_{ab}B_{bc}C_{ca}\,\delta(\omega_1+E_{ab})\,\delta(\omega_3+E_{ca}),$$

$$\rho^{II} = Z^{-1}(2\pi)^2 \sum_{a,b,c} e^{-\beta E_a} A_{ba}B_{cb}C_{ac}\,\delta(\omega_1+E_{ba})\,\delta(\omega_3+E_{ac}), \tag{7-19}$$

then it follows from the definitions of the ρ's that

$$\rho_{12} = e^{-\beta\omega_1}\rho^{I} + e^{\beta\omega_1}\rho^{II},$$

$$\rho_{23} = e^{\beta\omega_3}\rho^{I} + e^{-\beta\omega_3}\rho^{II},$$

$$\rho_{31} = \rho^{I} + \rho^{II}. \tag{7-20}$$

The cuts for $K(\omega_1, \omega_2, \omega_3)$ as a function of two complex variables are easily read off from the spectral representation (7-18). They are along

$$\text{Im } \omega_1 = 0, \text{ Im } \omega_2 = 0, \text{ and Im } \omega_3 = 0 .$$

These cuts divide the space into six regions as shown in Fig. 26. However, one of the cuts is missing for each of the three terms in (7-18). Figures 27a,b,c show the cuts for the three terms. Missing cuts are denoted by dashed lines.

C. Spectral Functions in Terms of the Discontinuities

The spectral functions can be found, when $K(\omega_1, \omega_2, \omega_3)$ is known, from the various discontinuities across the cuts. With the aid of (7-18) and Fig. 27, we find

$$\begin{aligned} K^1 - K^2 - K^5 + K^4 &= \rho_{12} - \rho_{31} \equiv \Delta_1 , \\ K^3 - K^4 - K^1 + k^6 &= \rho_{23} - \rho_{12} \equiv \Delta_2 , \\ K^2 - K^3 - K^6 + K^5 &= \rho_{31} - \rho_{23} \equiv \Delta_3 . \end{aligned} \tag{7-21}$$

The superscript on K denotes the regions of definition shown in Figs. 26,27. Only two of these three equations are independent. Also

$$\Delta_1 + \Delta_2 + \Delta_3 = 0 . \tag{7-22}$$

In terms of the functions ρ^I and ρ^{II} defined in (7-20), we obtain

$$\Delta_1 = \rho^I(e^{-\beta\omega_1} - 1) + \rho^{II}(e^{\beta\omega_1} - 1) \quad ,$$

$$\Delta_2 = \rho^I(e^{\beta\omega_3} - e^{-\beta\omega_1}) + \rho^{II}(e^{-\beta\omega_3} - e^{\beta\omega_1}) \quad ,$$

$$\Delta_3 = \rho^I(1 - e^{\beta\omega_3}) + \rho^{II}(1 - e^{-\beta\omega_3}) \quad . \tag{7-23}$$

Only two of the three equations are independent. Solving any two of these three for ρ^I and ρ^{II}, we have

$$\rho^I = [\Delta_1(e^{-\beta\omega_3} - 1) + \Delta_3(e^{\beta\omega_1} - 1)] /D \, ,$$

$$\rho^{II} = [\Delta_1(1 - e^{\beta\omega_3}) + \Delta_3(1 - e^{-\beta\omega_1})]/D \, , \tag{7-24}$$

where

$$D = e^{\beta\omega_1} + e^{\beta\omega_2} + e^{\beta\omega_3} - e^{-\beta\omega_1} - e^{-\beta\omega_2} - e^{-\beta\omega_3}$$

$$= (e^{\beta\omega_1} - 1)(E^{\beta\omega_2} - 1)(e^{\beta\omega_3} - 1) \, . \tag{7-25}$$

Once ρ^I, and ρ^{II} are known, ρ_{31}, ρ_{12}, ρ_{23} may be obtained from (7-20):

$$\rho_{ij} = [\Delta_i(e^{\beta\omega_j} - e^{-\beta\omega_j}) - \Delta_j(e^{\beta\omega_i} - e^{-\beta\omega_i})]/D \, ,$$

$$ij = 12, 23, 31 \, . \tag{7-26}$$

VIII. THE INTENSITY CORRELATION

The intensity correlation function of photons has been defined in Chapter II (see (2-2)). Its simplest physical interpretation is the probability of finding two photons, one at the space time point y_1, and one at y_2 :

$$\langle (A^+_\alpha(y_1)\, A^+_\beta(y_2))_- (A_\beta(y_2)\, A_\alpha(y_1))_+ \rangle$$

$$= \left\langle \sum_f |\langle f| (A_\beta(y_2)\, A_\alpha(y_1))_+ |s\rangle|^2 \right\rangle$$

averaged over the statistical ensemble of the states $|s\rangle$, which contains full information about the source.

In this chapter, we shall apply the temperature Green's function method to calculate the intensity correlation function. We first derive its connection with a particular temperature Green's function. This temperature Green's function can be obtained through the diagram method or through other means. As will be seen, within the framework of the diagram method, there can only be two terms for the intensity correlation function, i.e., the familiar direct term and the exchange term.

A. Connection with the Three End Temperature Green's Function

The photon intensity correlation function has been expressed in terms of the current correlation function J by (3-3,4) :

$$\langle \left(A^{\dagger}_{\alpha}(y_1)\, A^{\dagger}_{\beta}(y_2)\right)_{-} \left(A_{\beta}(y_2)\, A_{\alpha}(y_1)\right)_{+} \rangle$$

$$= \left[|g|^2\, V/(4\pi)^2\, y_1 y_2\right]^2 \int \frac{d\nu}{2\pi}\; J(\alpha\,\beta,\nu)$$

$$\times \exp - i\,\nu(t_2 - y_2 - t_1 + y_1) \quad ,$$

where

$$J(\alpha\,\beta,\nu)$$

$$= \int dt\; e^{i\nu t}\, \langle \left(j^{\dagger}_{\alpha}(\underset{\sim}{k})\; j_{\beta}(\underset{\sim}{k},t)\right)_{-} \left(j_{\beta}(\underset{\sim}{k},t)\; j_{\alpha}(\underset{\sim}{k})\right)_{+} \rangle \quad . \tag{8-1}$$

J can be written in terms of the matrix elements of the current operators between eigenstates of H as

$$J(\alpha\,\beta,\nu) = Z^{-1} \sum_{a,b,c} \left\{ j^{\dagger}_{\alpha ab}\, (j^{\dagger}_{\beta}\, j_{\beta})_{bc}\, j_{\alpha ca}\; \frac{e^{-\beta E_a}}{-i(\nu + E_{bc}) + \eta} \right.$$

$$\left. + \; j^{\dagger}_{\beta ab}\, (j^{\dagger}_{\alpha} j_{\alpha})_{bc}\, j_{\beta ca}\; \frac{e^{-\beta E_a}}{-i(\nu + E_{bc}) + \eta} \right\}$$

$$= \int \frac{d\nu'}{2\pi} \left\{ \frac{J'(\alpha\beta,\nu')}{-i(\nu - \nu') + \eta} + \frac{J'(\beta\,\alpha,\nu')}{i(\nu - \nu') + \eta} \right\}, \tag{8-2}$$

where

$$J'(\alpha\,\beta,\nu) = Z^{-1} \sum_{a,b,c} j^{\dagger}_{\alpha ab} (j^{\dagger}_{\beta}\, j_{\beta})_{bc}\, j_{\alpha ca}\, e^{-\beta E_a}\, 2\pi\, \delta(\nu + E_{bc}) \,. \tag{8-3}$$

$J'(\alpha\,\beta,\nu)$ may be obtained from a temperature Green's function with three ends. To see this, let us rewrite here the first expression in (7-19) for ρ^{I} :

$$\rho^{I} = Z^{-1}(2\pi)^2 \sum_{a,b,c} e^{-\beta E_a}\, A_{ab} B_{bc} C_{ca}\, \delta(\omega_1 + E_{ab})\, \delta(\omega_2 + E_{bc}) \,. \tag{8-4}$$

We have replaced $\delta(\omega_3 + E_{ca})$ in (7-19) by $\delta(\omega_2 + E_{bc})$. This is permissible since $\omega_1 + \omega_2 + \omega_3 = 0$ and hence

$$\begin{aligned} &\delta(\omega_1 + E_{ab})\, \delta(\omega_3 + E_{ca}) \\ &= \delta(\omega_1 + E_{ab})\, \delta(\omega_1 + E_{ab} + \omega_3 + E_{ca}) \\ &= \delta(\omega_1 + E_{ab})\, \delta(\omega_2 + E_{bc}) \,. \end{aligned} \tag{8-5}$$

If we let

$$\begin{aligned} A &= j^{\dagger}_{\alpha}(\underset{\sim}{k}) \,, \\ B &= j^{\dagger}_{\beta}(\underset{\sim}{k})\; j_{\beta}(\underset{\sim}{k}) \,, \\ C &= j_{\alpha}(\underset{\sim}{k}) \,, \\ \omega_2 &= \nu \,, \end{aligned} \tag{8-6}$$

and integrate over ω_1 , we obtain (8-3), i.e.,

$$J'(\alpha\,\beta,\omega_2) = \int \frac{d\omega_1}{2\pi}\ \rho^I(\omega_1,\omega_2) \quad .$$

ρ^I may be obtained from (7-24) in terms of Δ_1 and Δ_3 , the discontinuities of K . After some rearrangements, we find

$$J'(\alpha\,\beta,\ \nu) = \frac{1}{e^{\beta\nu} - 1} \int \frac{d\omega}{2\pi} \left(\frac{\Delta_3}{e^{\beta\omega} - 1} + \frac{\Delta_1}{e^{\beta\omega} - e^{-\beta\nu}} \right) , \tag{8-7}$$

where Δ_1 and Δ_2 are evaluated at

$$\omega_1 = -\nu - \omega \ ,$$

$$\omega_2 = \nu \ ,$$

$$\omega_3 = \omega \ . \tag{8-8}$$

Thus we have established the connection between the temperature Green's function K and the desired correlation function. K is represented diagramatically in Fig. 28. (See Section V.B for the conventions regarding diagramatic representations. The current operators are defined by (3-7). The dotted line indicates that the operators $j^{\dagger}_{\beta}(\underset{\sim}{k})$ and $j_{\beta}(\underset{\sim}{k})$, which are obtained from $j^{\dagger}_{\beta}(\underset{\sim}{x})$ and $j_{\beta}(\underset{\sim}{x}')$ by separate Fourier transforms and whose product is the B operator (see (8-6)), are separated in space although they are tied to the same time.

The remaining task is to find the temperature Green's function K and feed the results into (8-7).

B. The Direct Term and the Exchange Term

There are two disconnected diagrams contributing to K (see Figs. 29,30). First, consider the direct term given by Fig. 29 :

$$K_{dir}(\omega_1,\omega_2,\omega_3) = \langle j^\dagger_\beta\, j_\beta\rangle \;\mathcal{G}(-\omega_1)\,\beta\,\delta_{\omega_2,0} \quad . \tag{8-9}$$

$\langle j^\dagger_\beta\, j_\beta\rangle$ is simply $\mathcal{G}$ with ends tied together:

$$\langle j^\dagger_\beta\, j_\beta\rangle = \frac{1}{\beta}\sum_{\omega'} \mathcal{G}(\omega')\, e^{\eta\omega'}$$

$$= \int \frac{d\omega'}{2\pi}\;\frac{1}{e^{\beta\omega}-1}\;\left(\mathcal{G}(\omega'+i\eta)-\mathcal{G}(\omega'-i\eta)\right)$$

$$= \int \frac{d\omega'}{2\pi}\; S(\omega') \equiv S_T \quad . \tag{8-10}$$

S_T may be called the total source strength. The power spectrum $S(\omega)$ is given by (5-3) in terms of $\mathcal{G}(\omega)$.

To analytically continue K_{dir} , we write $\beta\,\delta^K(\omega_2)$ for $\beta\,\delta_{\omega_2,0}$ (see (4-17,17') and the discussion there):

$$K_{dir}(\omega_1,\omega_2,\omega_3) = S_T\;\mathcal{G}(-\omega_1)\,\beta\,\delta^K(\omega_2) \tag{8-11}$$

which is discontinuous across $\mathrm{Im}\,\omega_1 = 0$, and $\mathrm{Im}\,\omega_2 = 0$. The discontinuities are obtained from (7-21):

$$\Delta_1 = (e^{\beta\omega_1} - 1)\ S_T\ [\mathcal{D}(-\omega_1 - i\eta)] - \mathcal{D}(-\omega_1 + i\eta]$$

$$\times\ \beta[\delta^K(\omega_2 + i\eta) - \delta^K(\omega_2 + i\eta)]$$

$$= (e^{\beta\omega_2} - 1)\ S_T\ S(-\omega_1)\ (e^{-\beta\omega_1} - 1)\ \alpha\pi\ \delta(\omega_2)\ , \qquad (8\text{-}12)$$

and $\Delta_3 = 0$.

Substituting (8-12) in (8-7) taking into account (8-8), we have the expected result:

$$J'_{dir}\ (\alpha\beta,\nu) = 2\pi\ \delta(\nu)\ S_T^{\,2}\ . \qquad (8\text{-}13)$$

Next, consider the <u>exchange term</u> given by Fig. 30 :

$$K_{exc}\ (\omega_1,\omega_2,\omega_3) = \mathcal{D}(\omega_3)\ \mathcal{D}(-\omega_1)\ \delta_{\alpha\beta}\ , \qquad (8\text{-}14)$$

which has cuts along $\mathrm{Im}\ \omega_3 = 0$ and along $\mathrm{Im}\ \omega_1 = 0$.

By (7-21),

$$\Delta_1 = [-\mathcal{D}(\omega_3 + i\eta) + \mathcal{D}(\omega_3 - i\eta)]\ [-\mathcal{D}(-\omega_1 + i\eta) + \mathcal{D}(-\omega_1 - i\eta)]\ \delta_{\alpha\beta}$$

$$= -(e^{\beta\omega_3} - 1)\ (e^{-\beta\omega_1} - 1)\ S(\omega_3)\ S(-\omega_1)\ \delta_{\alpha\beta}\ ,$$

$$\Delta_3 = {}^{*}\Delta_1\ . \qquad (8\text{-}15)$$

Substituting (8-15) in (8-7) taking (8-8) into account, we obtain the simple result

$$J'_{exc}(\alpha\beta,\nu) = \int \frac{d\omega}{2\pi} S(\omega) S(\omega+\nu) \delta_{\alpha\beta} . \qquad (8\text{-}16)$$

Figures 29, 30 are the only disconnected diagrams contributing to K. In the limit of large volume, connected diagrams are negligible compared to the disconnected diagrams because each connected piece implies a factor of volume. Within the framework of diagram method, we must keep only the terms with the highest power of volume because Wick's theorem is meaningful only in the limit of an infinite volume. Therefore, within the limit of applicability of the diagram method, (8-13,16) give the exact result.

Substituting (8-13,16) into (8-2,1) we obtain the result

$$\langle (A^{\dagger}_{\alpha}(y_1) A^{\dagger}_{\beta}(y_2))_{-} (A_{\beta}(y_2) A_{\alpha}(y_1))_{-} \rangle = [S_T|g|^2 V/(4\pi)^2 y_1 y_2]^2$$

$$\times \left[1 + \delta_{\alpha\beta} \left| \int \frac{d\omega}{2\pi} e^{-i\omega(t_2-y_2-t_1+y_1)} s(\omega) \right|^2 \right] , \qquad (8\text{-}17)$$

where $s(\omega)$ is the normalized power spectrum defined by

$$s(\omega) \equiv S(\omega)/S_T . \qquad (8\text{-}18)$$

All the information about the source is contained in the power spectrum $S(\omega)$, which we have discussed in detail in Chapters V and VI. It is clear that the intensity correlation function contains no more information about the source than the amplitude correlation function.

IX. SUMMARY AND DISCUSSION

The over-all picture of our analysis is the following. The photon field is coupled to the many atom source system. The correlations in the many atom system lead to the correlations in the photon field. The influence of the photon field back on the source is ignored. After the correlations in the photon field are written in terms of the correlations in the source system, the latter are then studied by the temperature Green's function method regarding the source system as a large many body interacting system. In connection with the power spectrum, we have studied in some detail the behavior of the many atom source model. We have also analyzed various properties of temperature Green's functions in general.

Our study has demonstrated the power of the diagrammatic temperature Green's function method of analysis. Indeed, this method is mathematically rigorous and straightforward. The very complicated process of averaging a product of Heisenberg operators at different times is reduced to the elegant procedure of analytic continuation and simple diagram rules.

Our analysis also reflects the limitation of the diagrammatic temperature Green's function technique. This technique is limited to systems in thermal equilibrium. The price for the diagram rules is the restriction of the analysis to infinite systems. More important, the physical meaning of the analytic continuation procedure and that of more complicated diagrams are not transparent. As has been stated in Chapter III, the limitation of the method limits the validity of our results to special cases.

The expression for the intensity correlation function derived in Chapter VIII (see (8-17)) agrees with that derived through other methods (see, for example, Ref. 2). Through the expressions of photon correlation functions in terms of the correlations in the source system, one can obtain information concerning the latter by experimentally analyzing the former. A detailed discussion in this connection can be found in Ref. 2.

The formulation in this thesis applies to a solid or a liquid source, too. The mathematical procedure would be essentially the same. In a solid or in a liquid, the correlations are described in terms of the propagation of various elementary excitations (such as electrons, holes, excitons) and the interactions among them. When the temperature is not too high, the elementary excitations behave very much like the particles in a dilute gas.

Lasers are light sources of current interest. Unfortunately, a temperature cannot be defined for the laser cavity. While the populations of the internal states are inverted and describable by a negative temperature, the kinetic energy of the atoms and the interactions among them must be described by a positive temperature. As was mentioned before, the temperature Green's function method applies only to a system with a single positive temperature. The generalization of the method to systems not in thermal equilibrium is expected to be non-trivial.

ACKNOWLEDGMENTS

I would like to express my gratitude to Professor Kenneth M. Watson for his constant guidance, encouragement and support. I am grateful to Professor Eyvind H. Wichmann for his criticism and suggestions.

I would like to thank Dr. Loren Meissner for his advice and help in programming. Thanks are also due to Dr. Harvey Gould for many helpful discussions.

This work was done under the auspices of the United States Atomic Energy Commission.

APPENDICES

A. The Photon-Atom Coupling

Since the size of an atom is much smaller than the wavelength of an optical photon, the atoms may be regarded as point particles. For optical transitions, the A^2 term in the usual electromagnetic coupling is not effective. The interaction

$$\mathcal{H}(x) = g\, A^{+}_{\mu}(x)\, j_{\mu}(x) + \text{h.c.} \qquad \text{(A-1)}$$

is adequate. j_{μ} changes the state of the atom from the upper level to the lower level. j^{+}_{μ} does the opposite.

We now derive the expressions (2-5) and (2-6). We do it here in order to make the main text simpler and more continuous.

Let $|i\rangle$ be the state, in the interaction picture, of the system (source plus the vacuum outside) at the time $-\infty$, and let $U(t,t')$ be the time displacement operator in the interaction picture. We shall put a prime to an operator to denote that operator in the interaction picture. The un-primed operators are in the Heisenberg picture.

The state of the system at time $t = 0$ is

$$|s\rangle = U(0, -\infty)\, |i\rangle \ .$$

Thus,

$$A_\mu(y)|s\rangle = U(0,t)\, A'_\mu(y)\, U(t,-\infty)|i\rangle$$

$$= U(0,t)\, [A'_\mu(y),\, U(t,-\infty)]|i\rangle \quad . \tag{A-2}$$

We have set $A'_\mu(y)|i\rangle$ to zero, i.e., the photons created before the time $-\infty$ are ignored.

Since

$$U(t,-\infty) = \left(\exp - i \int_{-\infty}^{t} d^4x\, \mathcal{H}'(x)\right)_+ \quad , \tag{A-3}$$

and

$$[A'_\mu(y),\, \mathcal{H}'(x)] = g[A'_\mu(y)\, A'^{+}_\nu(x)]\, j'_\nu(x) \quad , \tag{A-4}$$

we have

$$U(0,t)[A'_\mu(y),\, U(t,-\infty)] = -ig \int d^4x\; D_{\mu\nu}(y-x)$$

$$\times\, U(0,t)\left(j'_\nu(x) \exp - i \int d^4x'\; \mathcal{H}'(x')\right)_+$$

$$= -ig \int d^4x\, D_{\mu\nu}(y-x)\, j_\nu(x)\, U(0,-\infty) \quad , \tag{A-5}$$

where

$$D_{\mu\nu}(y-x) \equiv [A'_\mu(y),\, A'^{+}_\nu(x)]\, \theta(t-\tau) \tag{A-6}$$

$$= (\delta_{\mu\nu} - \hat{k}_\mu \hat{k}_\nu)\, \theta(t-\tau) \int \frac{d^3k}{(2\pi)^3}\, \frac{1}{2k}\, e^{i\underset{\sim}{k}\cdot(\underset{\sim}{y}-\underset{\sim}{x}) - ik(t-\tau)} \quad . \tag{A-7}$$

Therefore, (A-2) becomes

$$A_\mu(y)|s\rangle = -ig\int d^4x\ D_{\mu\nu}(y-x)\ j_\nu(x)|s\rangle\ . \qquad \text{(A-8)}$$

It follows that

$$\langle s|\ A^+_\alpha(y_1)\ A_\beta(y_2)|s\rangle$$

$$= |g|^2\int d^4x_1 d^4x_2\ D^*_{\alpha\mu}(y_1-x)\ D_{\beta\nu}(y_2-y_2)\ \langle s|\ j^\dagger_\mu(x_1)\ j_\nu(x_2)|s\rangle\ . \qquad \text{(A-9)}$$

Averaging over an ensembe of $|s\rangle$, we obtain (2-5).

Applying another photon annihilation operator to both sides of (A-2), we obtain, letting $t_2 > t_1$ for the moment,

$$\left(A_\beta(y_2)\ A_\alpha(y_1)\right)_+|s\rangle$$

$$= U(0,t_2)\ A'_\beta(y_2)\ U(t_2,t_1)\ [A'_\alpha(y_1),\ U(t,-\infty)]|i\rangle$$

$$= U(0,t_2)\ \left[A'_\beta(y_2),\ U(t_2,t_1)\ [A'_\alpha(y_1),\ U(t,-\infty)]\right]\ |i\rangle\ . \qquad \text{(A-10)}$$

Similar to (A-5), (A-10) can be written in terms of the current operators. Since j'_μ and A'_μ commute, (A-10) becomes, by (A-3,4),

$$\left(A_\beta(y_2)\, A_\alpha(y_1)\right)_+ |s\rangle$$

$$= U(0,t_2)\cdot(-g^2)\int d^4x_2\, d^4x_1\, D_{\beta\nu}(y_2 - x_2)\, D_{\alpha\mu}(y_1 - x_1)$$

$$\times \left(j'_\nu(x_2)\, j'_\mu(x_1) \exp - i \int_{-\infty}^{t_2} d^4x\, \mathcal{H}'(x)\right)_+ |i\rangle$$

$$= -g^2 \int d^4x_2\, d^4x_1\; D_{\beta\nu}(y_2 - x_2)\, D_{\alpha\mu}(y_1 - x_1)$$

$$\times \left(j_\nu(x_2)\, j_\mu(x_1)\right)_+ |s\rangle \quad . \qquad \text{(A-11)}$$

By the same argument, one arrives at (A-11) for $t_2 < t_1$. Squaring (A-11) and averaging over the ensembe of $|s\rangle$, one obtains (2-6) .

B. Numerical Procedure

The integral equation (6-27) to be solved is:

$$\phi'(\underset{\sim}{y},\lambda) = \left(\lambda - \underset{\sim}{y}\cdot\hat{k} - \tilde{\Sigma}'(y) - \Sigma'(y)\right)^{-1} \times \left[1 + \int d^3y'\, F'(\underset{\sim}{y},\underset{\sim}{y}')\, \phi'(\underset{\sim}{y},\lambda)\right] , \qquad \text{(B-1)}$$

with the restriction that

$$\int d^3y\, e^{-y^2}\, \phi'(\underset{\sim}{y},\lambda)$$

shall be finite.

Equation (B-1) can be solved by approximating the integral by a finite sum so that the integral equation becomes a set of simultaneous linear equations of the form, in matrix notation,

$$AC = B \ . \qquad \text{(B-2)}$$

C is then obtained by matrix division:

$$C = A^{-1} B \ .$$

The matrix division can be done in a reasonable amount of time on the newest machine only if the dimensionality of A is smaller than about 100. The integral in (B-1) can be reduced to a two dimensional

integral by exploiting the cylindrical symmetry. However, it is still impossible to well approximate the integral by a sum over 100 mesh points. Therefore, we expand the function $\phi'(\underset{\sim}{y},\lambda)$ in a series of Legendre and Laguerre polynomials:

$$\phi'(\underset{\sim}{y},\lambda) = \sum_{\ell,n} C_{\ell n}(2\ell + 1)\,(4\pi)^{-1}\,P_\ell(x) \times L_n(y^2) \quad , \tag{B-4}$$

where $x \equiv \hat{k}\cdot\hat{y}$, and then truncate the series. We expect $\phi'(\underset{\sim}{y},\lambda)$ to be a smooth function of $\underset{\sim}{y}$ so that terms of high order are negligible. The motivation of using $L_n(y^2)$ is that there are many integrals over e^{-y^2} to do.

The kernal $F'(\underset{\sim}{y},\underset{\sim}{y}')$ is a function of y,y' and $\hat{y}\cdot\hat{y}' \equiv x'$. It can therefore be written as

$$F'(\underset{\sim}{y},\underset{\sim}{y}') = \sum_{\ell} (2\ell + 1)\,(4\pi)^{-1}\,P_\ell(x')\,F_\ell(y,y') \quad ,$$

where

$$F_\ell(y,y') = 2\pi \int_{-1}^{1} dx'\,F'(\underset{\sim}{y},\underset{\sim}{y}') \quad . \tag{B-5}$$

The integral equation (B-1) now becomes a set of linear equations for the coefficients $C_{\ell n}$:

$$\sum_{\ell',n'} A_{\ell n,\ell' n'} C_{\ell' n'} = B_{\ell n} , \qquad \text{(B-6)}$$

where

$$A_{\ell n,\ell' n'} = \delta_{\ell\ell'} \delta_{nn'} - 2\pi \int_0^\infty e^{-y^2} dy^2 \; L_n(y^2)$$

$$\times (2\ell' + 1)(4\pi)^{-1} \int_{-1}^{1} dx \; P_\ell(x) P_{\ell'}(x)/D(y,x)$$

$$\times \frac{1}{2} \int_0^\infty dy'^2 \cdot y' F_{\ell'}(y,y') L_{n'}(y'^2) ,$$

$$B_{\ell n} = 2\pi \int_0^\infty dy^2 \, e^{-y^2} L_n(y^2) \int_{-1}^{1} dx \; P_\ell(x)/D(y,x) ,$$

$$D(y,x) = \lambda - yx - \tilde{\Sigma}'(y) - \Sigma'(y) . \qquad \text{(B-7)}$$

The integral (6-33) is

$$S'(\lambda) = \int d^3y \; e^{-y^2} \; \phi'(y,\lambda)$$

$$= \frac{1}{2} \sum_n C_{0n} \int_0^\infty dy^2 \, e^{-y^2} \; y \, L_n(y^2) . \qquad \text{(B-9)}$$

We keep Legendre polynomials of order less than 6 and Laguerre polynomials of order less 4 . Then (B-6) is a set of 24 linear equations. These equations were solved and the sum (B-9) computed for various input parameters on a Control Data 6600 computer.

FOOTNOTES AND REFERENCES

1. M. Born and E. Wolf, Principles of Optics (Pergamon Press, New York, 1959), Chapter X.

2. M. L. Goldberger and K. M. Watson, Phys. Rev. 137, B1396 (1965).

3. R. J. Glauber, Phys. Rev. 131, 2766 (1963).

4. For a review of the field, see R. G. Breene, Jr., The Shift and Shape of Spectral Lines (Pergamon Press, New York, 1961).

5. J. W. Bond, Jr., K. M. Watson, and J. A. Welch, Jr., Atomic Theory of Gas Dynamics (Addison-Wesley, Reading, Massachusetts, 1965), pp. 150-154.

6. A. A. Abrikosov, L. P. Gordov and I. E. Dzyerloshinski, Methods of Quantum Field Theory in Statistical Physics (Prentice Hall, Inc., Englewood Cliffs, New Jersey, 1963), Chapter 3.

7. E. J. Squires, Complex Angular Momentum and Particle Physics, (W. A. Benjamin, Inc., New York, 1963), p. 3.

8. This is a standard procedure. See T. Holstein, Ann. Phys. 29, 410 (1964), or G. M. Eliashberg, JETP 14, 886 (1962).

9. B. D. Fried and S. D. Conte, The Plasma Dispersion Fuction (Academic Press, 1961).

10. R. H. Dicke, Phys. Rev. 89, 472 (1953).

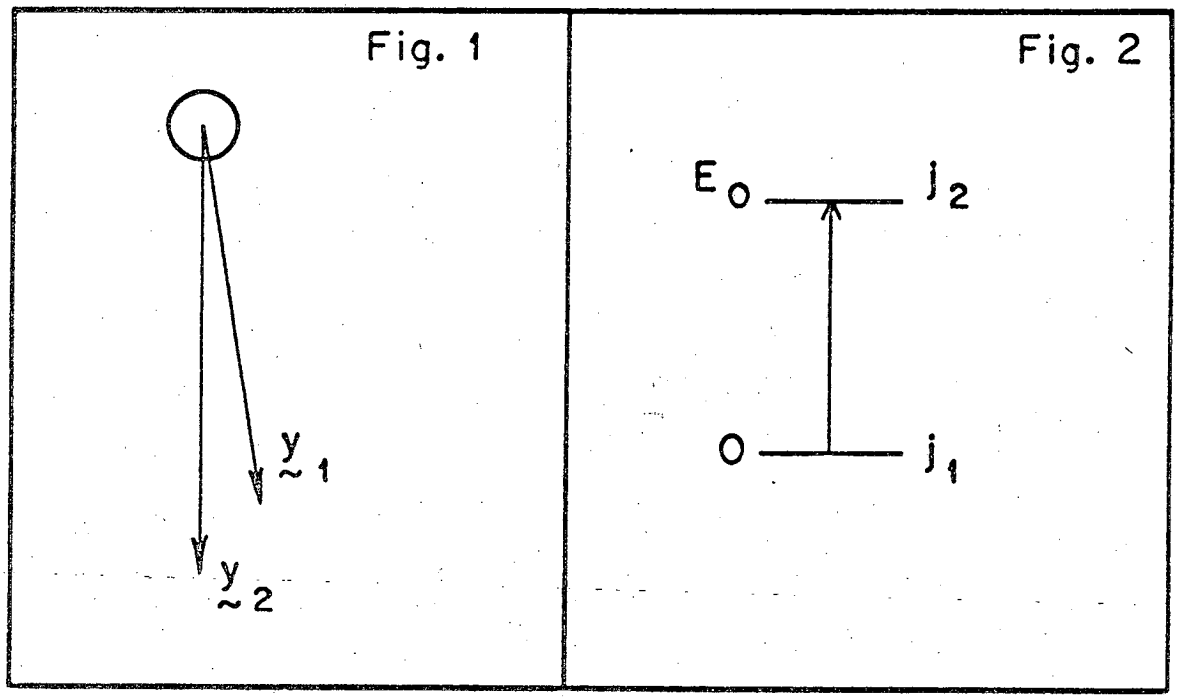

MUB-10606

Fig. 1. (See Section III-A.) The source and the observation points.

Fig. 2. (See Section III-B.) The two atomic levels of interest. The degeneracies of the two levels are $2j_1 + 1$ and $2j_2 + 1$, respectively. The unperturbed energy differences is E_0.

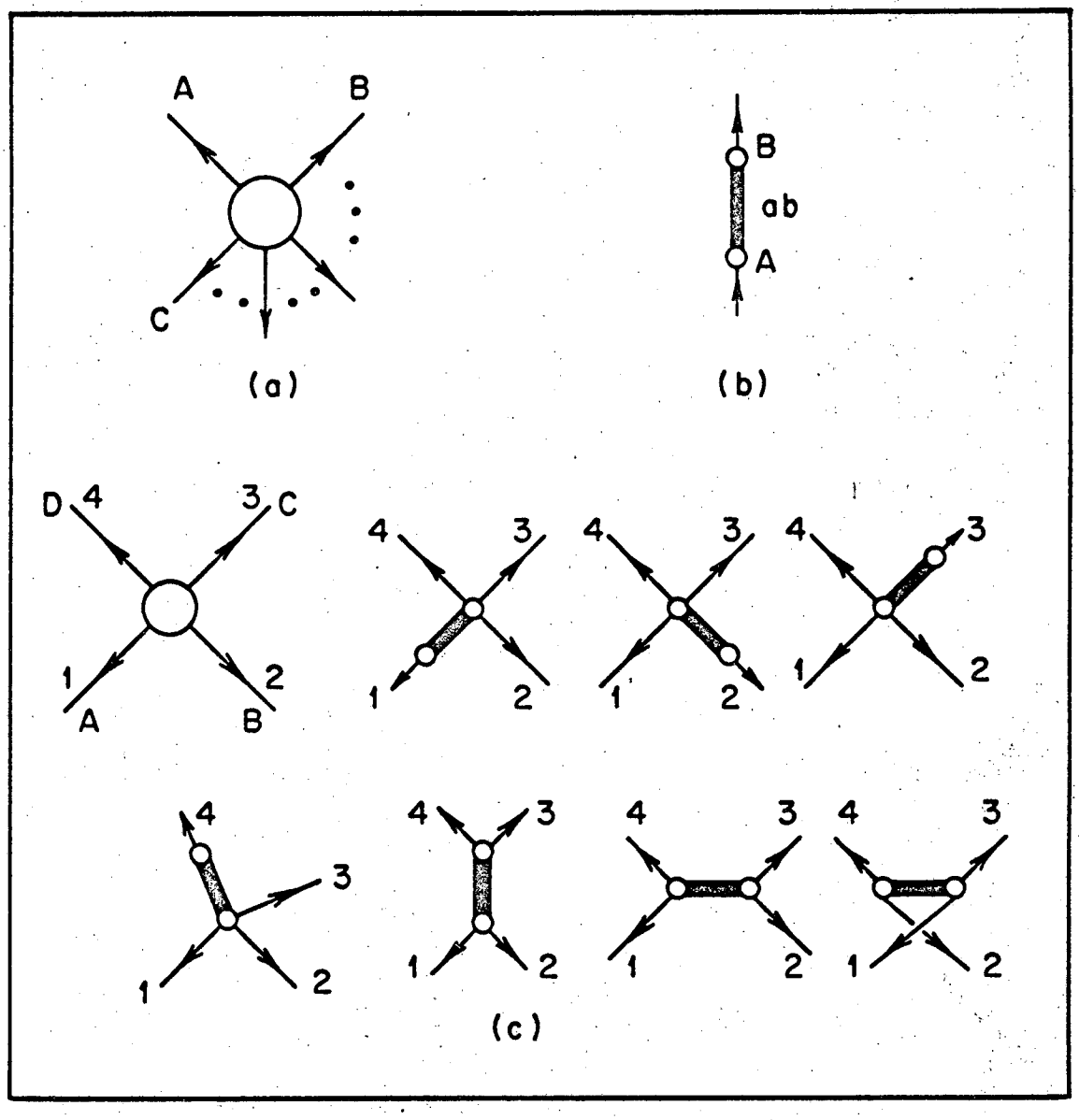

MUB-10607

Fig. 3. (See Subsection IV-C-2.) a. Schematic representation of a general temperature Green's function.
b. The schematic representation of a term in the expansion of a temperature Green's function of two ends (see (4-9, 11,12)).
c. A general four end temperature Green's function. The seven elementary excitation lines (the very thick lines) give rise to seven cuts.

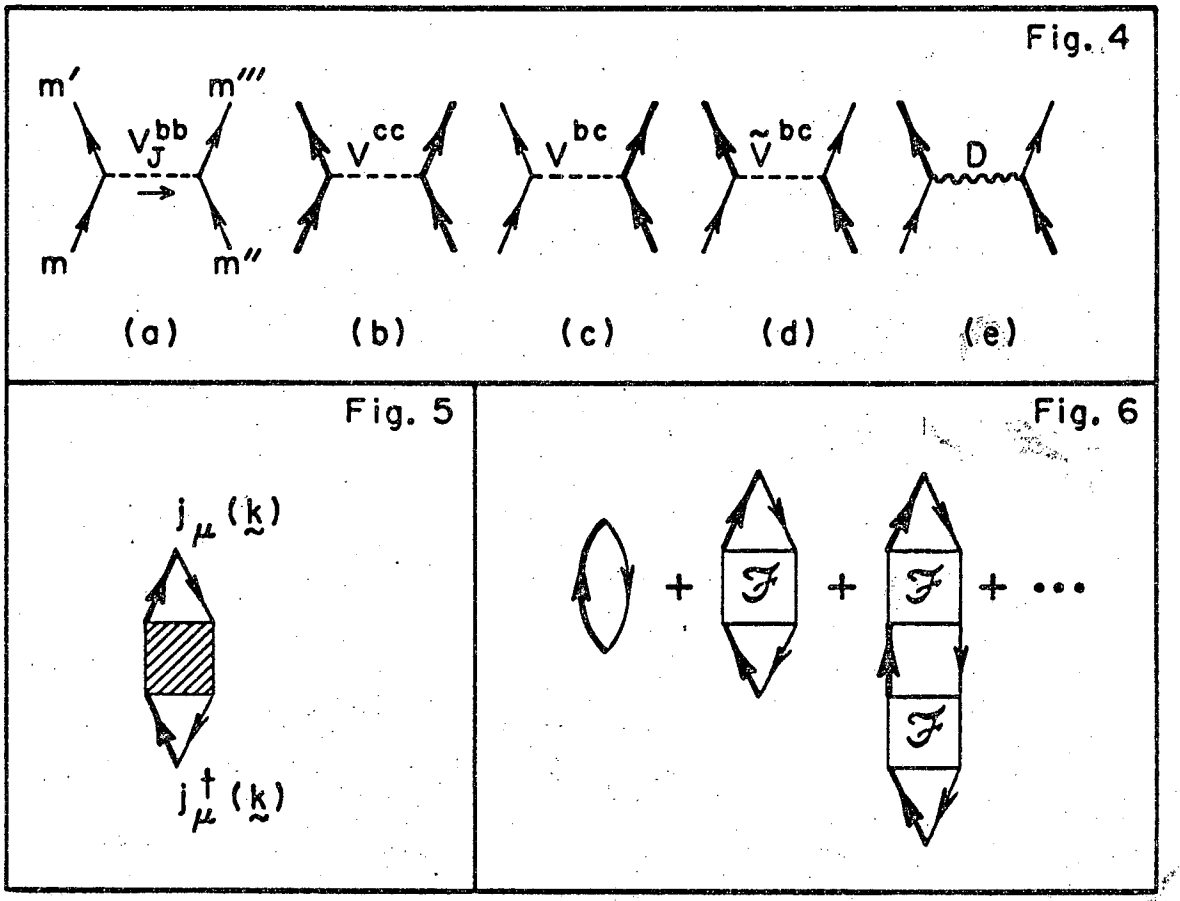

MUB-10608

Fig. 4. (See Section III-C.) Momentum and spin are transferred from one atom to another. The thick lines (thin lines) represent atoms in the upper (lower) level. The wavy line in (e) represents a virtual photon. (a), (b), (c) represent elastic scatterings. (d) and (e) represent scatterings with internal energy transfer.

Fig. 5. (See Section V-B.) The Green's function $\mathcal{G}$.

Fig. 6. (See Section V-B.) The Green's function $\mathcal{G}$ in Fig. 5 is broken into a sum. $\mathcal{F}$ cannot be broken further into two pieces connected by one thick line up and one thin line down.

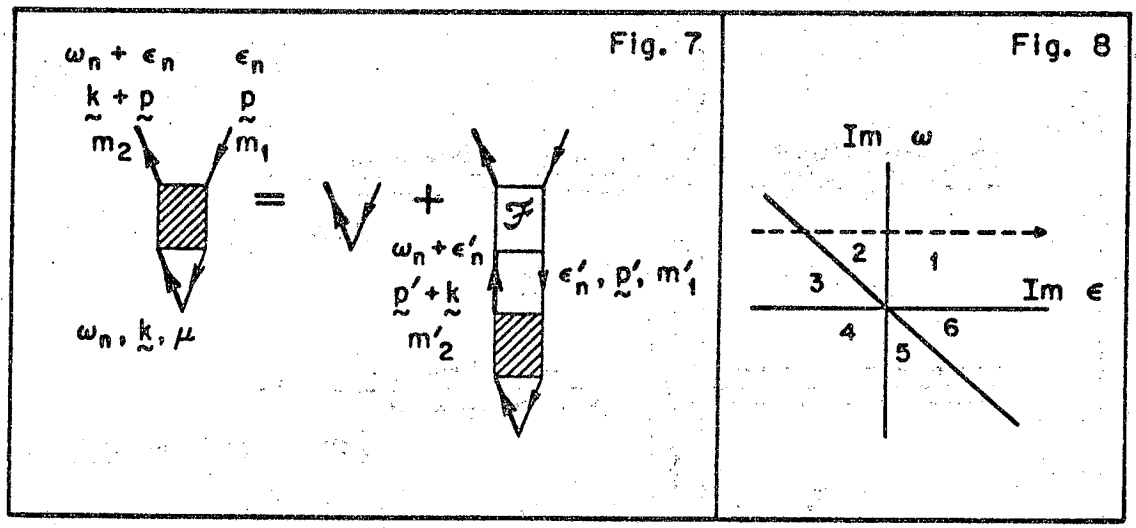

MUB-10609

Fig. 7. (See Section V-C.) The integral equation satisfied by the vertex function K .

Fig. 8. (See Section V-C.) The cuts of the analytically continued K . The dashed line represents the ϵ-plane shown in Fig. 9.

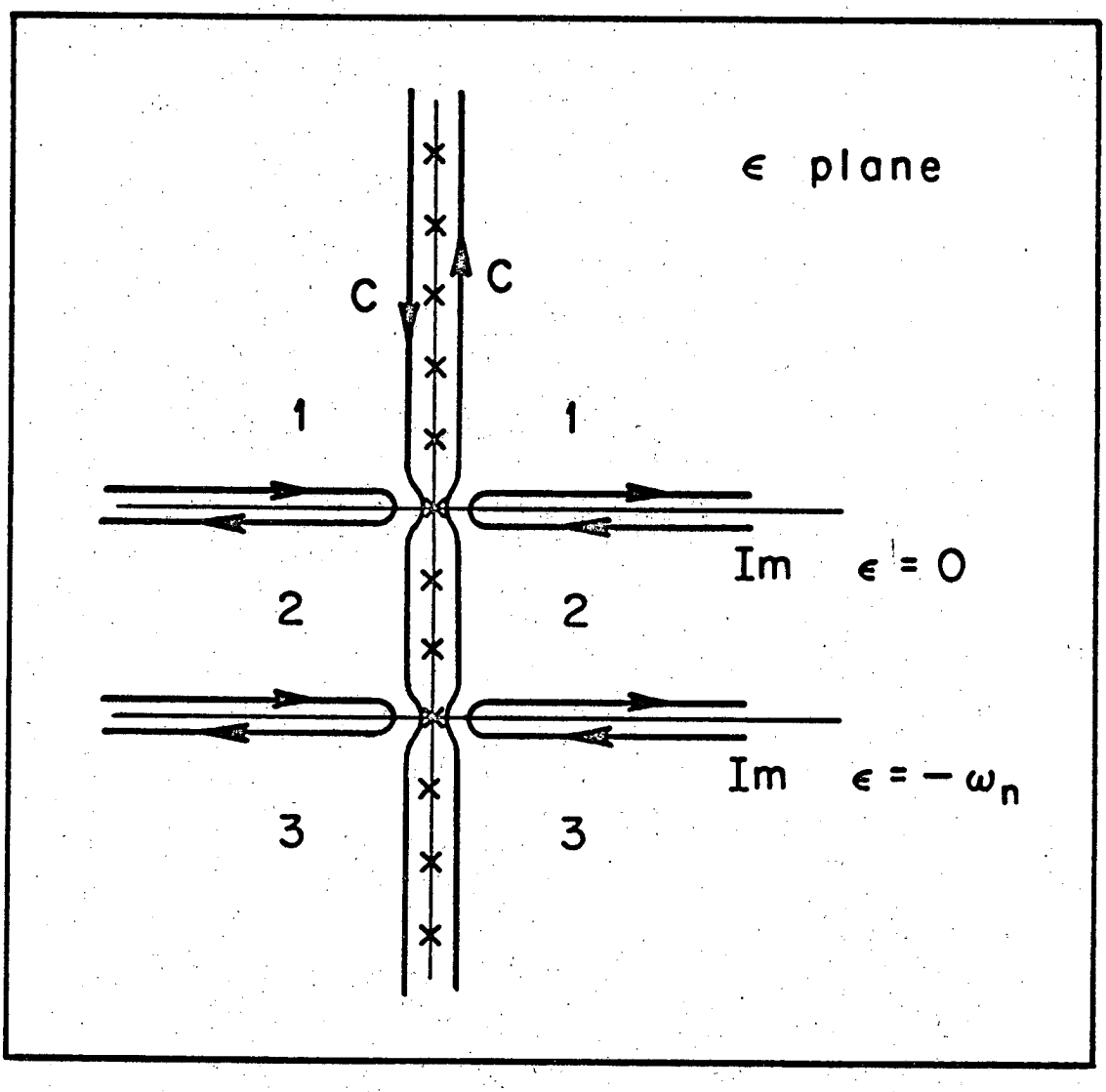

MUB-10610

Fig. 9. (See Section V-C.) The cuts of $K(\epsilon, \omega_n)$ on the ϵ-plane and the integration contours.

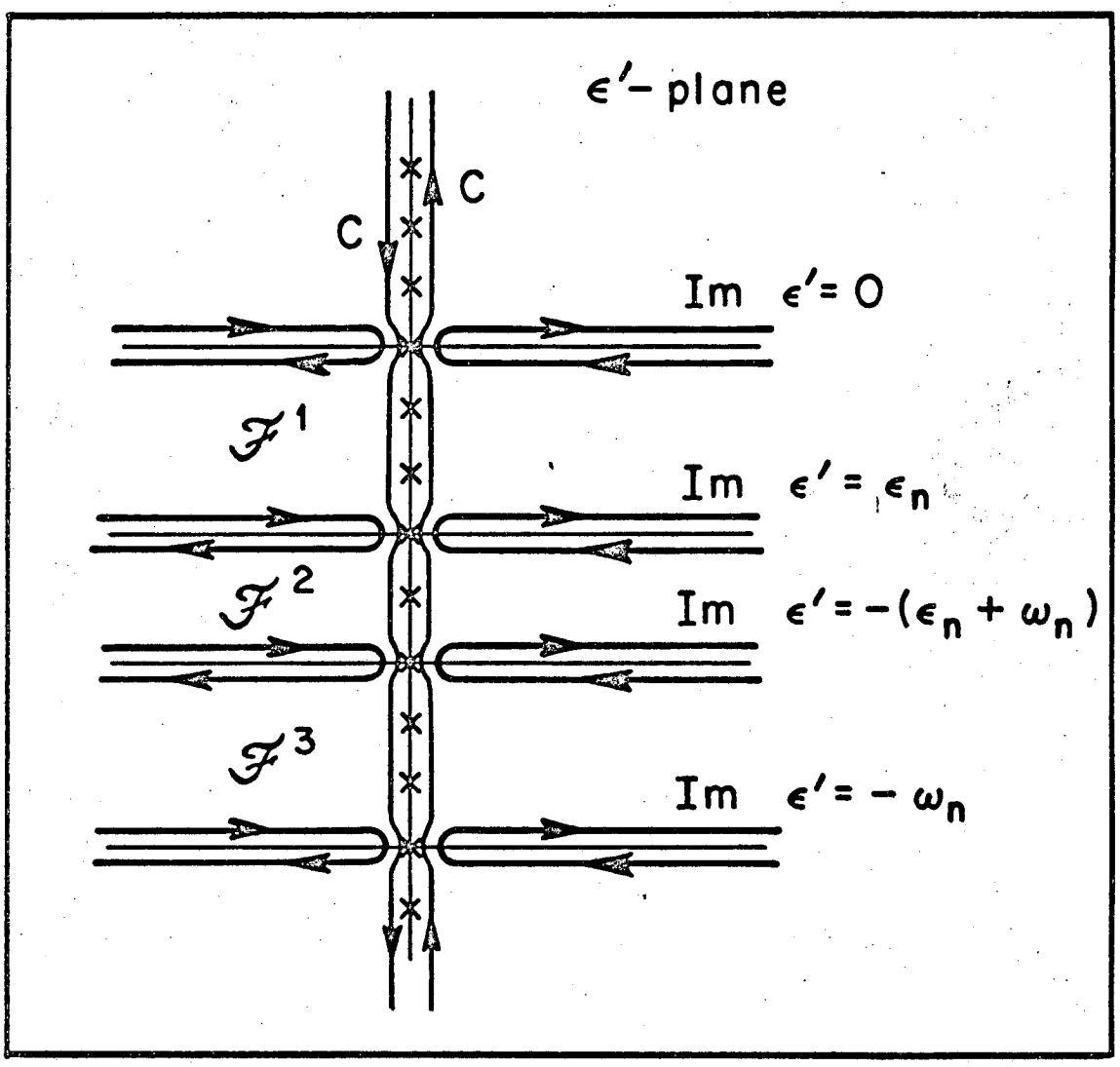

MUB-10611

Fig. 10. (See Section V-D.) The cuts of $\mathcal{F}(\epsilon_n, \epsilon', \omega_n)$ on the ϵ'-plane and the integration contours.

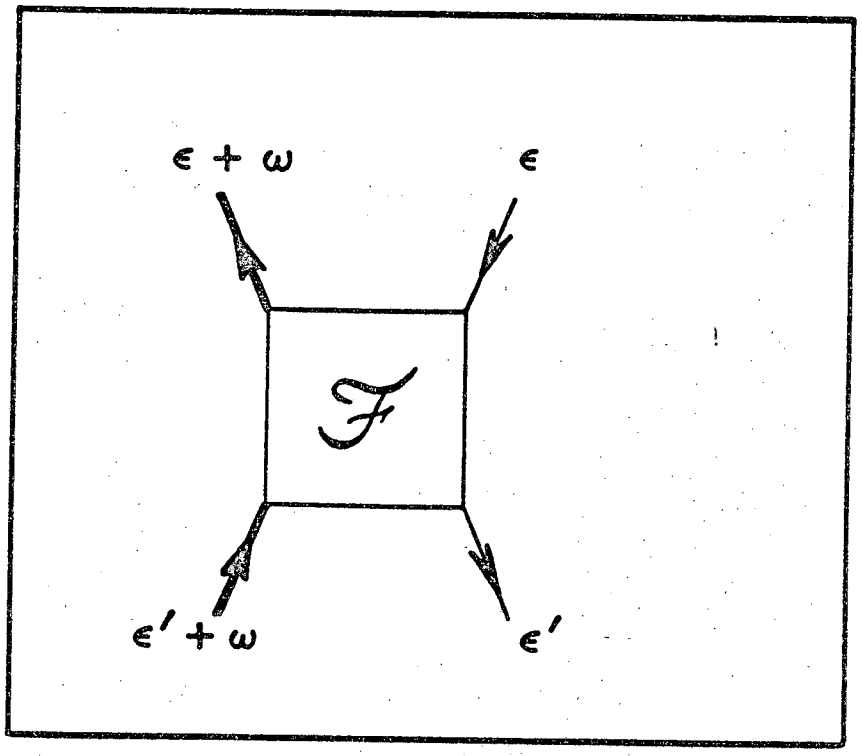

MUB-10612

Fig. 11. (See Section V-D.) The four corner function $\mathcal{F}$ hooked to four legs.

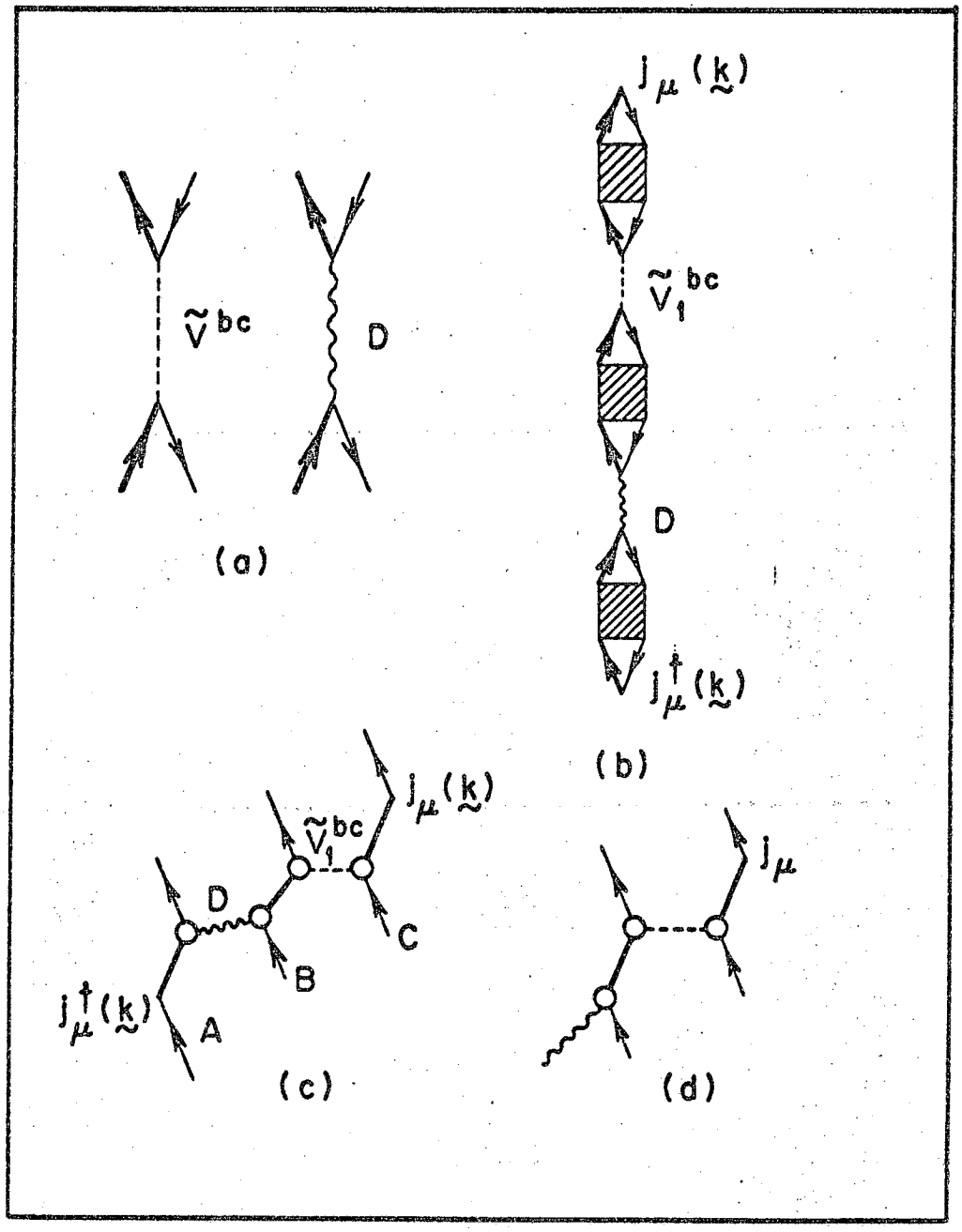

MUB-10613

Fig. 12. (See Section VI-A.) a. the lowest order contribution to the kernal $F(\underset{\sim}{p},\underset{\sim}{p}')$.

b. An example of the string diagrams generated by Fig. 12a.

c. The scatterings (the events between the operators j^+_μ and j_μ) transfer the internal energy of the atom A to the atom C.

d. A cavity mode quantum excites an atom, which transfers its internal energy to another atom. j_μ is the coupling to the photon field outside the source (see Section VI-B).

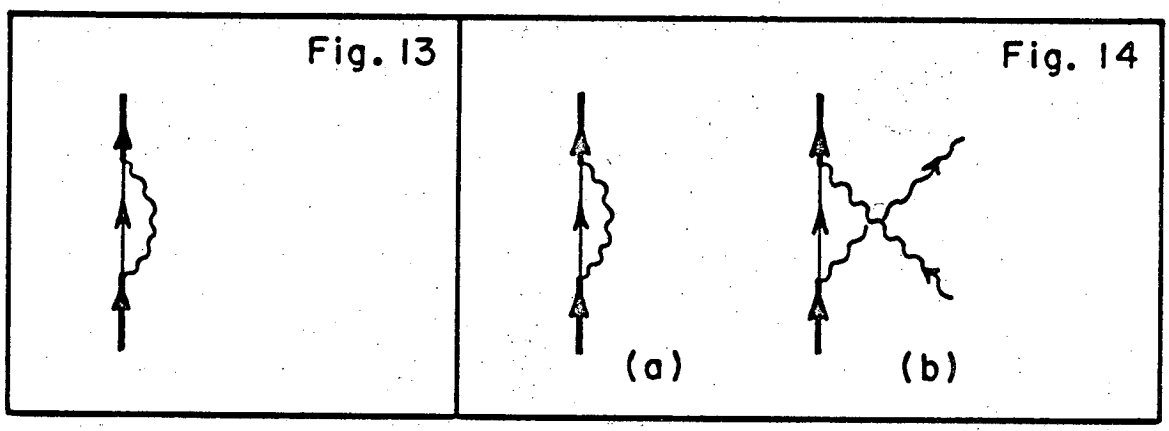

MUB-10614

Fig. 13. (See Section VI-A.) The self energy diagram due to the internal energy transfer via the exchange of a virtual photon.

Fig. 14. (See Section VI-A.) Figure 13 unscrambled.

(a) The temperature independent "true" self energy.

(b) The self energy due to scattering.

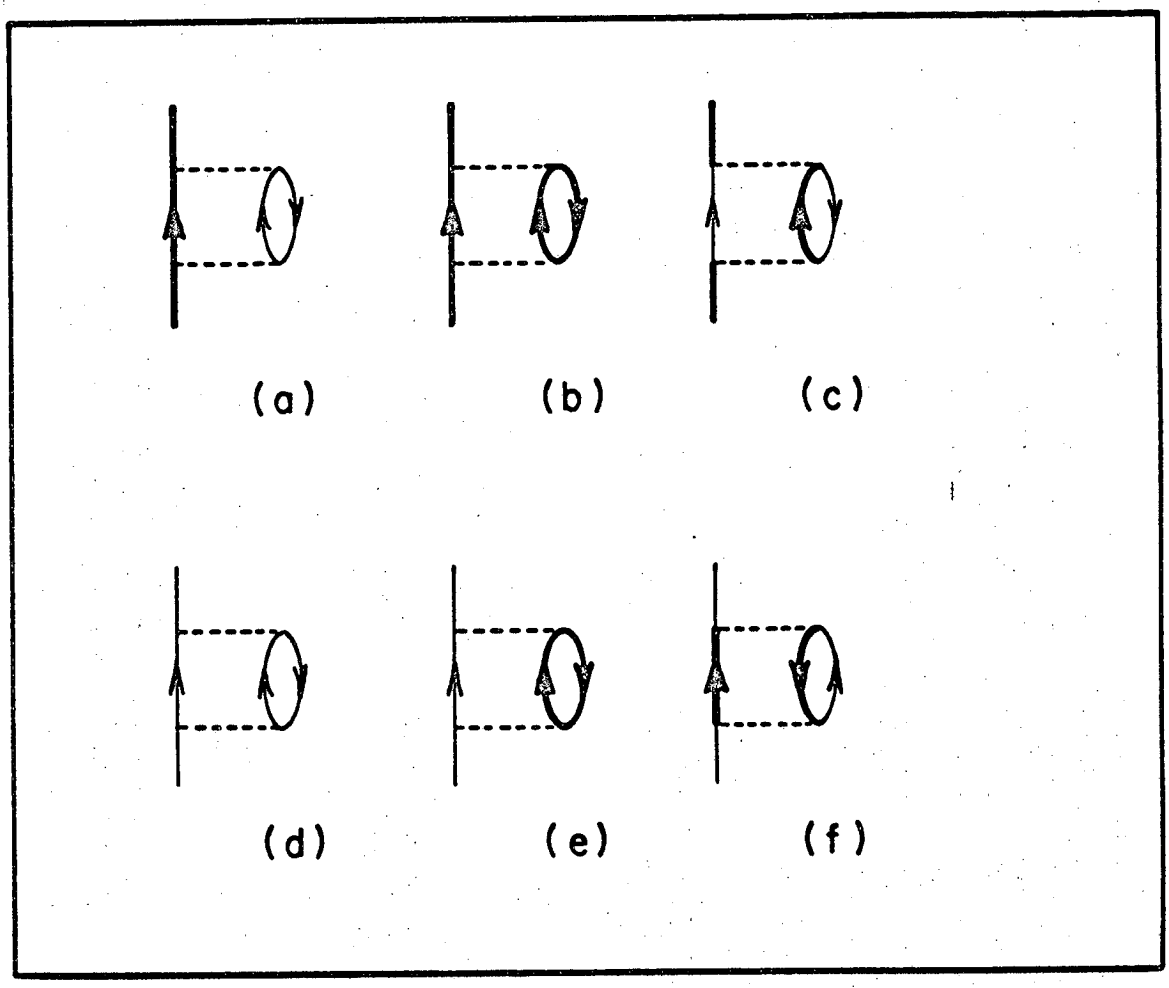

MUB-10615

Fig. 15. (See Section VI-C.) The second order self energy diagrams representing the terms (6-5,6).

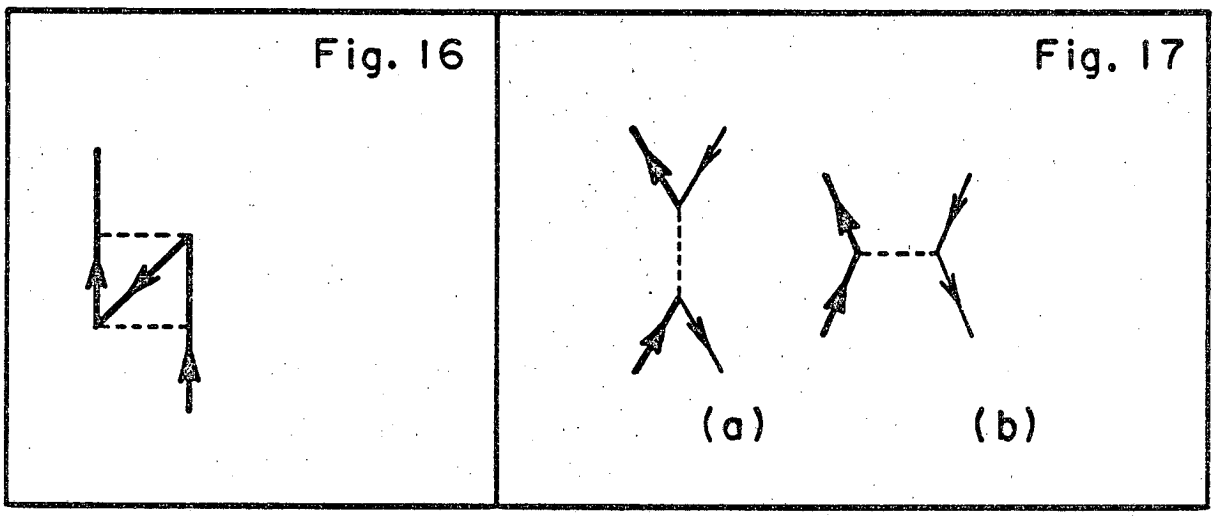

MUB-10616

Fig. 16. The exchange diagram obtained from Fig. 15b by switching the upper end of the line on the right and that on the left.

Fig. 17. (See Section VI-D.) First order contributions to $F(\underset{\sim}{p},\underset{\sim}{p}')$.

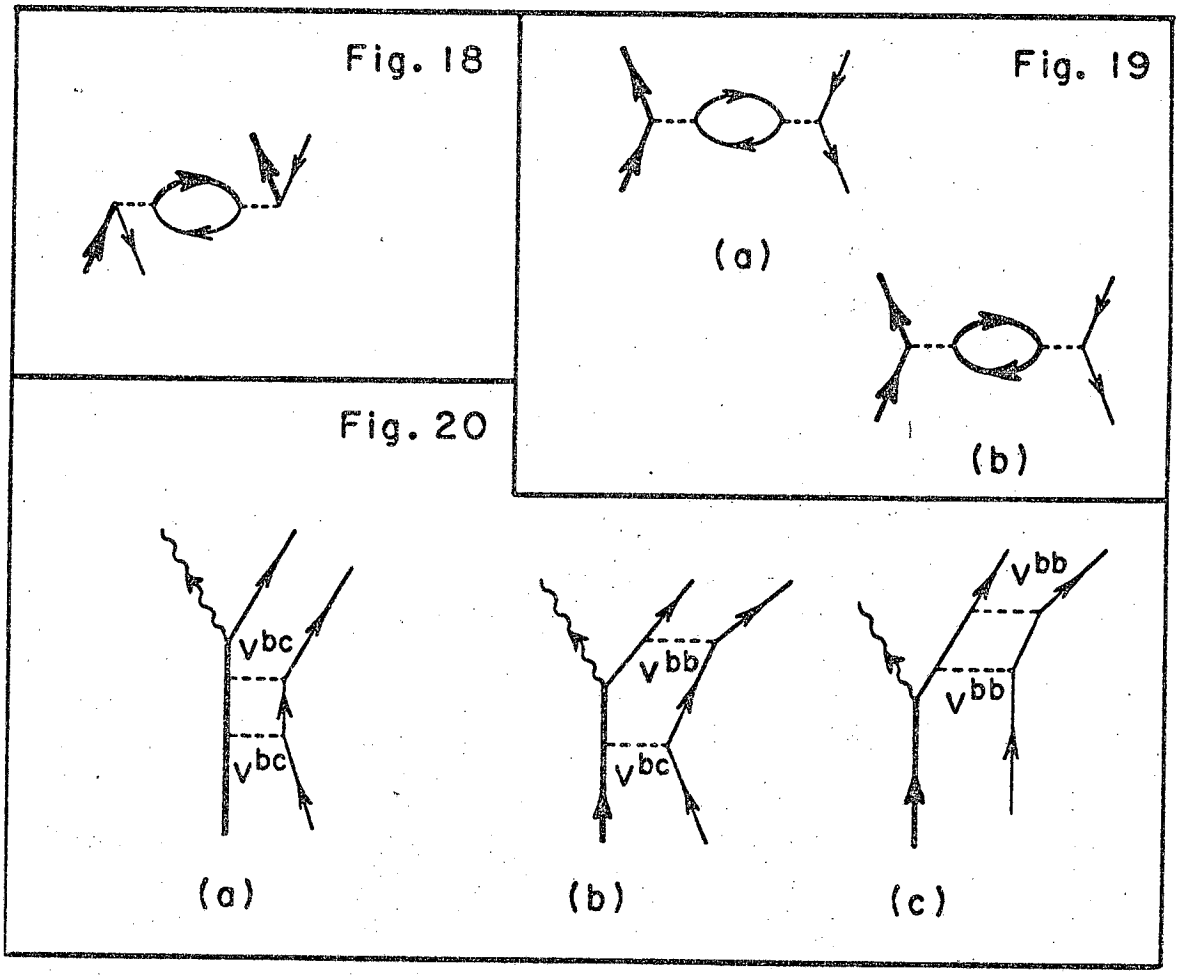

MUB-10617

Fig. 18. (See Section VI-D.) The effect of this diagram is included in the first order kernal.

Fig. 19. (See Section VI-D.) The second order diagrams representing the terms in (6-9).

Fig. 20. (See Section VI-D.) The second order elastic scattering of to atoms while a photon is being emitted.

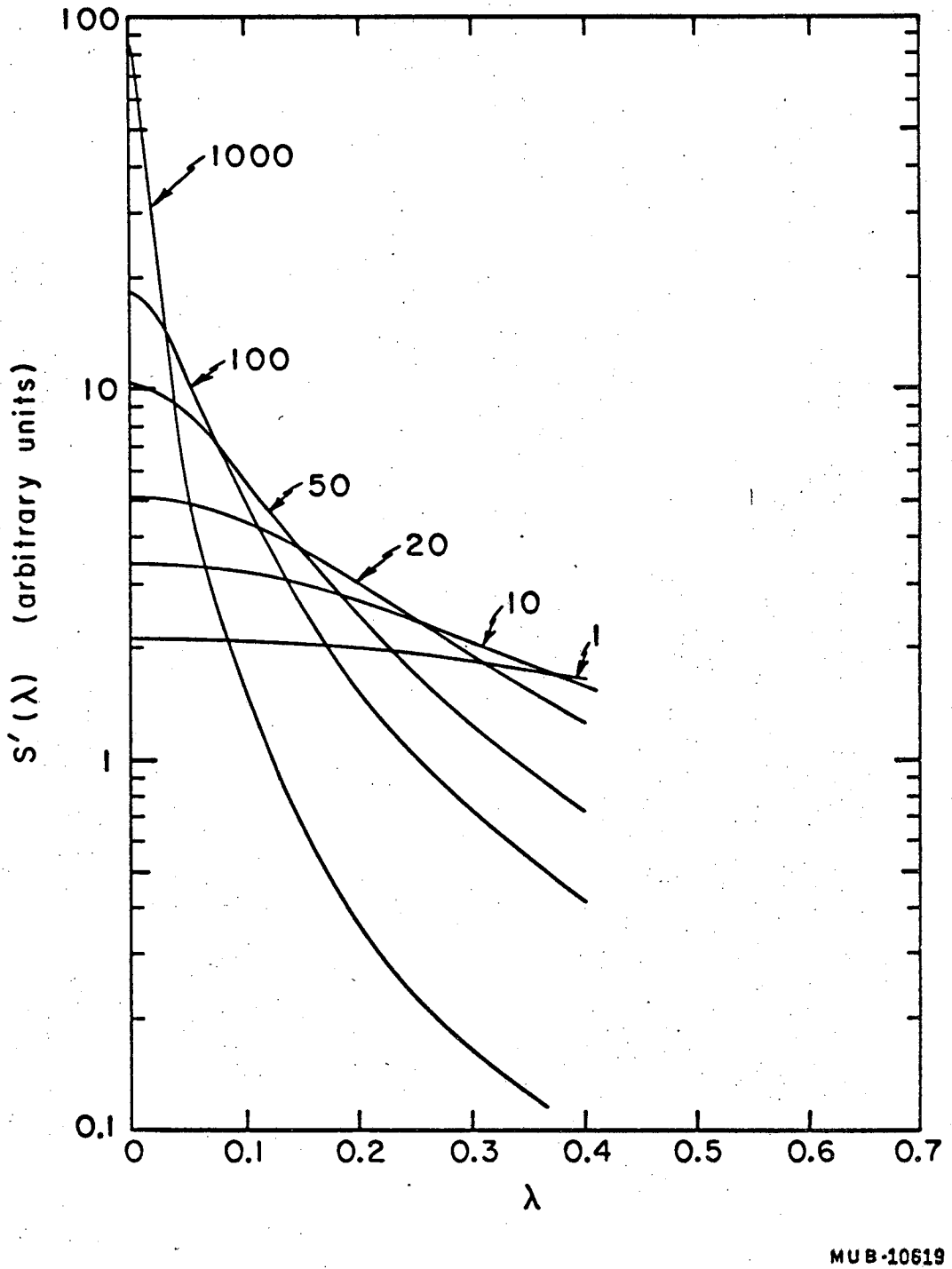

Fig. 21. (See Section VI-F.) The power spectrum $S'(\lambda)$ vs. λ (see (6-24,29,33) for the definition of the parameters). $\tilde{\xi}^{\pm} = 0$ for the curves in this figure. $S'(\lambda) = S'(-\lambda)$. The numbers labeling the curves are the values of ξ.

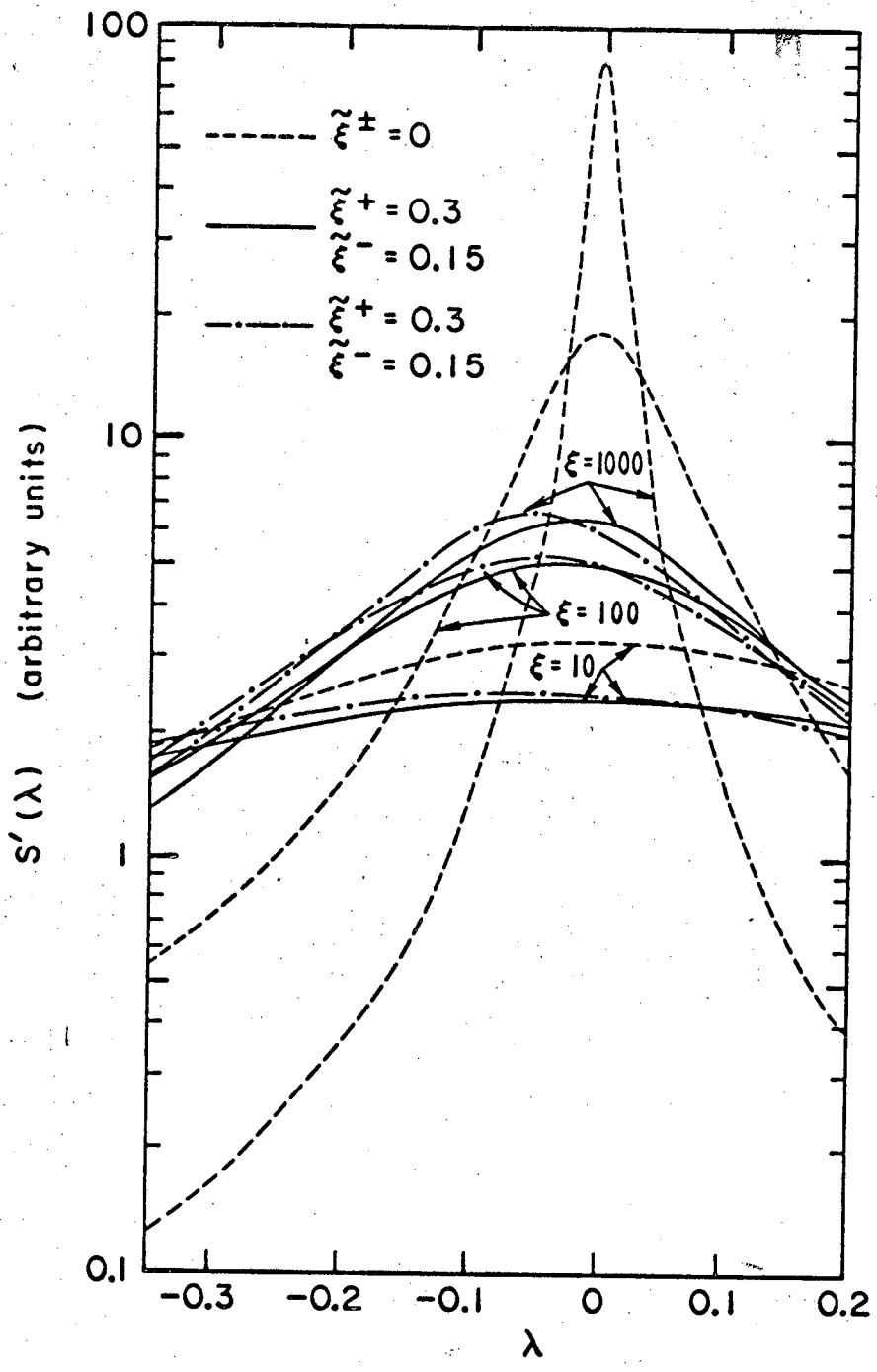

Fig. 22. (See Section VI-F.) The power spectrum vs. λ. The dashed curves are the reproductions of the curves in Fig. 21 for ξ = 10,100, 1000 for comparison.

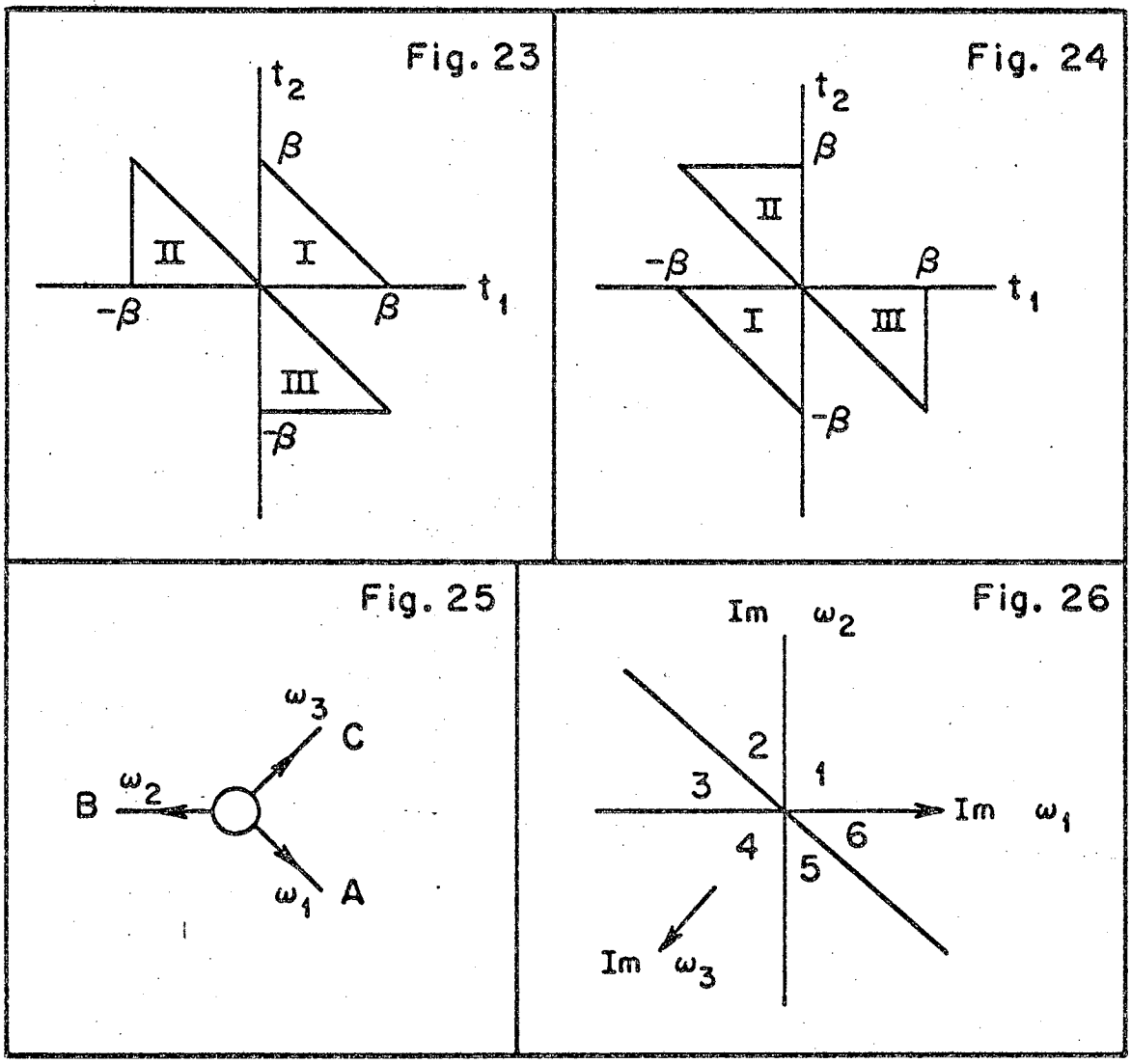

MUB-10620

Fig. 23. (See Section VII-A.) Domains of definition of K(Cycle 1).

Fig. 24. (See Section VII-A.) Domains of definition of K(Cycle 2).

Fig. 25. (See Section VII-B.) Schematic representation of $K(\omega_1, \omega_2, \omega_3)$.

Fig. 26. (See Section VII-B.) The cuts for $K(\omega_1, \omega_2, \omega_3)$ in the space of two complex variables.

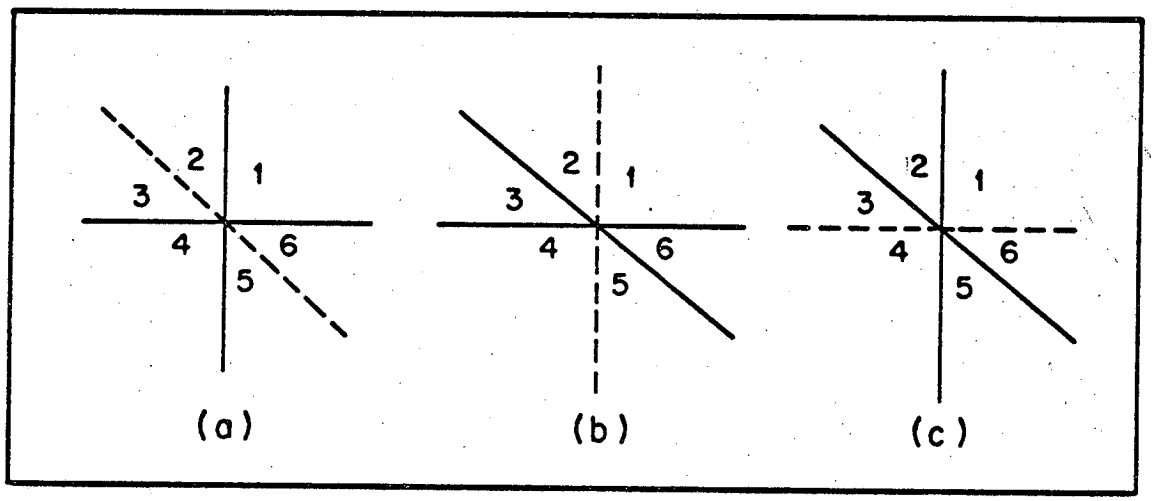

MUB-10621

Fig. 27. (See Section VII-B.) The cuts for the three terms in (7-18).

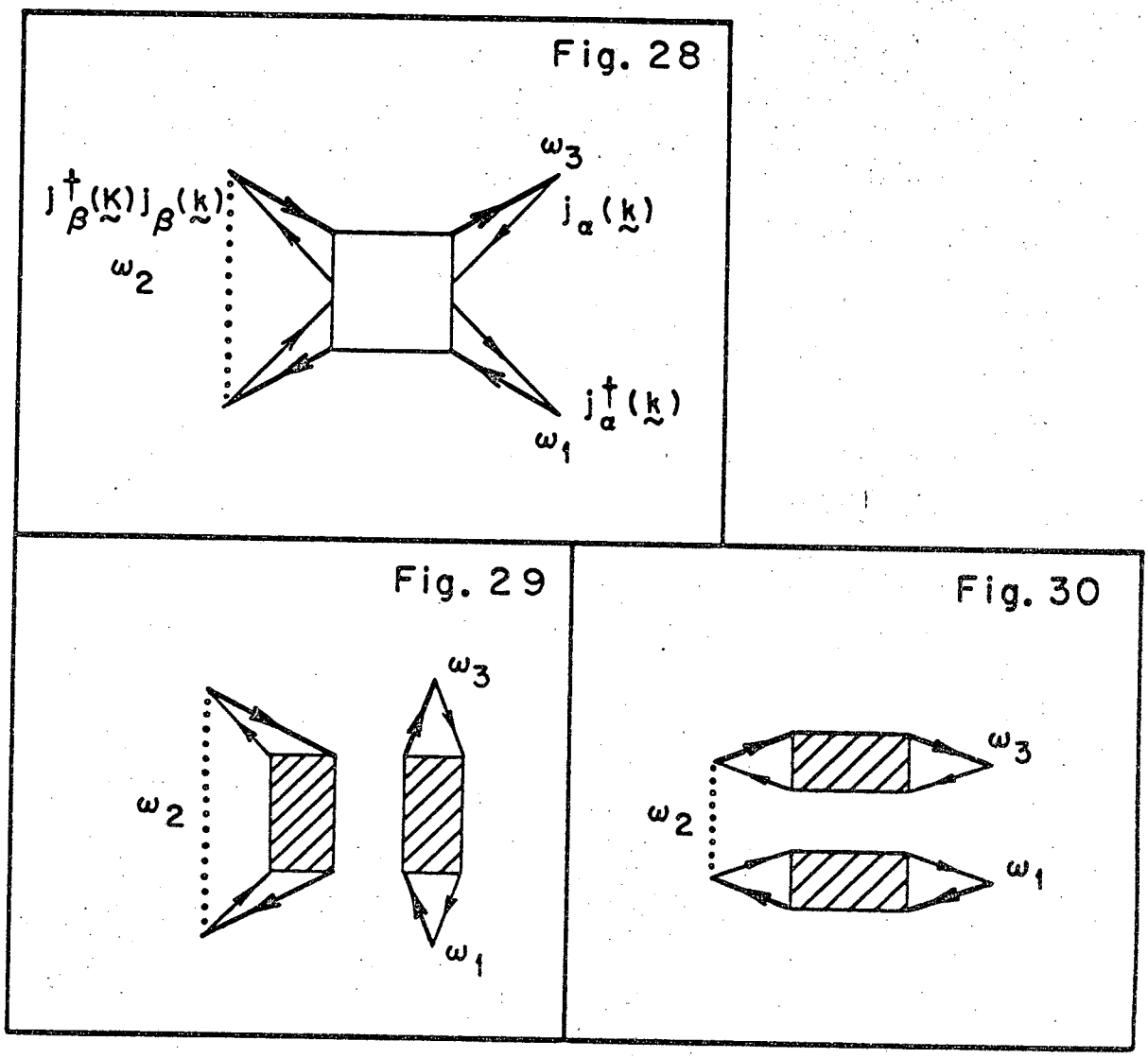

MUB-10622

Fig. 28. (See Section VIII-A.) The diagram representation of K. The dotted line indicates that j^+_β and j_β are tied to the same time.

Fig. 29. (See Section VIII-B.) The diagram leading to the direct term.

Fig. 30. (See Section VIII-B.) The diagram leading to the exchange term.